NASA-X-524-72-212
PREPRINT

NASA TM X-65946

THE BAPE II BALLOON-BORNE CO_2 LASER HETERODYNE EXPERIMENT

JUNE 1972

GSFC
GODDARD SPACE FLIGHT CENTER
GREENBELT, MARYLAND

X-524-72-212

THE BAPE II BALLOON-BORNE CO_2 LASER HETERODYNE EXPERIMENT

J. J. Degnan
H. E. Walker
C. J. Peruso
E. H. Johnson
B. J. Klein
J. H. McElroy

June 1972

GODDARD SPACE FLIGHT CENTER
Greenbelt, Maryland

CONTENTS (continued)

THE BAPE II BALLOON-BORNE CO_2 LASER HETERODYNE EXPERIMENT

1. INTRODUCTION

In September 1971, a CO_2 laser transmitter was flown on-board a series of high altitude research balloons launched from Holloman Air Force Base near Alamogordo, New Mexico as part of the BAPE II project. The primary purpose of BAPE II was to gather atmospheric propagation data using ground-based lasers and on-board detectors (reported elsewhere). The experiment also provided a rare opportunity to determine whether or not an air-to-ground CO_2 laser heterodyne link could be established using existing components which at that time had only been tested under controlled conditions This report is intended to familiarize LPE and ATS project members, potential contractors, and other interested parties with the systems and techniques utilized in this first attempt to establish an air-to-ground CO_2 laser heterodyne link and with the successes and problems encountered when the heterodyne receiver and laser transmitter package were removed from the controlled environment of the laboratory.

The report discusses four major topics:

1. A discussion of the existing systems and of the underlying principles involved in their operation;

2. An account of experimental techniques and optical alignment methods which were found to be useful in the field;

3. Theoretical calculations of signal strengths expected under a variety of test conditions and in actual flight; and

4. A discussion of the experimental results including problems encountered and their possible solutions.

2. INSTRUMENTATION

2.1 Telescope and Startracker Systems

A 76 cm diameter Cassegrainian telescope with an effective focal length of 1.15 m mounted on a standard tracking mount (not vibrationally isolated) served as the receiving antenna for the present experiment. A 4-watt Argon laser was mounted on a table inside a trailer adjacent to the tracking mount. The Argon beam, 100% modulated by a mechanical chopper at 5KHz entered a coelostat

and exited parallel to the scope axis from a tube whose center was displaced approximately 48 cm from the center of the receiving aperture. The Argon beam provided a ground-based beacon for the flight package startracker and its reflection off of cube corners on the package provided an Argon "star" for the ground-based startracker. The 5Khz modulation assisted the flight package startracker in distinguishing the beacon from the radiation background.

A cylinder on the flight package containing the CO_2 transmitter and the airborne startracker was capable of moving independently of the main bulk of the package. Power was supplied through slip rings from batteries mounted in the main structure. The azimuth and elevation pointing angles of the flight package were controlled by telemetry from the ground until the Argon beacon entered the 8 degree acquisition field-of-view of the on-board startracker. At this point, the startracker would take command of the servo systems and point the package at the ground-based beacon.

The startracker on the flight package consists of a detecting photodiode layer with a central contact at a negative potential with respect to four outer contacts equally spaced along the outer circumference of the detecting layer. The Argon light focused by the startracker optics onto the photodiode material produces conduction electrons which cause currents to flow through the outer contacts. Differences in the current generate pointing error signals which are used to drive the azimuth and elevation servo systems until all four currents are equalized.

When the on-board startracker is locked onto the beacon, the flight package cube corners are facing the ground station. A portion of the reflected beam is intercepted by the 76 cm diameter scope and focused on the ground-based startracker.

The ground-based startracker built by ITT consists of an optical lens, photosensor, and electronics. The lens system gathers and brings to focus radiant energy at the photocathode of an image dissector. The image dissector has a photocathode surface which forms an electron image of the focused image. It is constructed such that, when an accelerating voltage is applied between the photocathode and an internal mechanical limiting aperture, only electrons from a particular area of the cathode will pass through the limiting aperture (see Figure 2-1). This particular area is called the instantaneous photocathode area and when projected through the tracker lens, represents a region in space defined as the instantaneous field-of-view approximately equal to 6 arcseconds. Following the aperture is a secondary emission dynode structure providing signal amplification. A deflection coil is positioned around the image dissector to provide deflection of the electron image. By applying the proper deflection

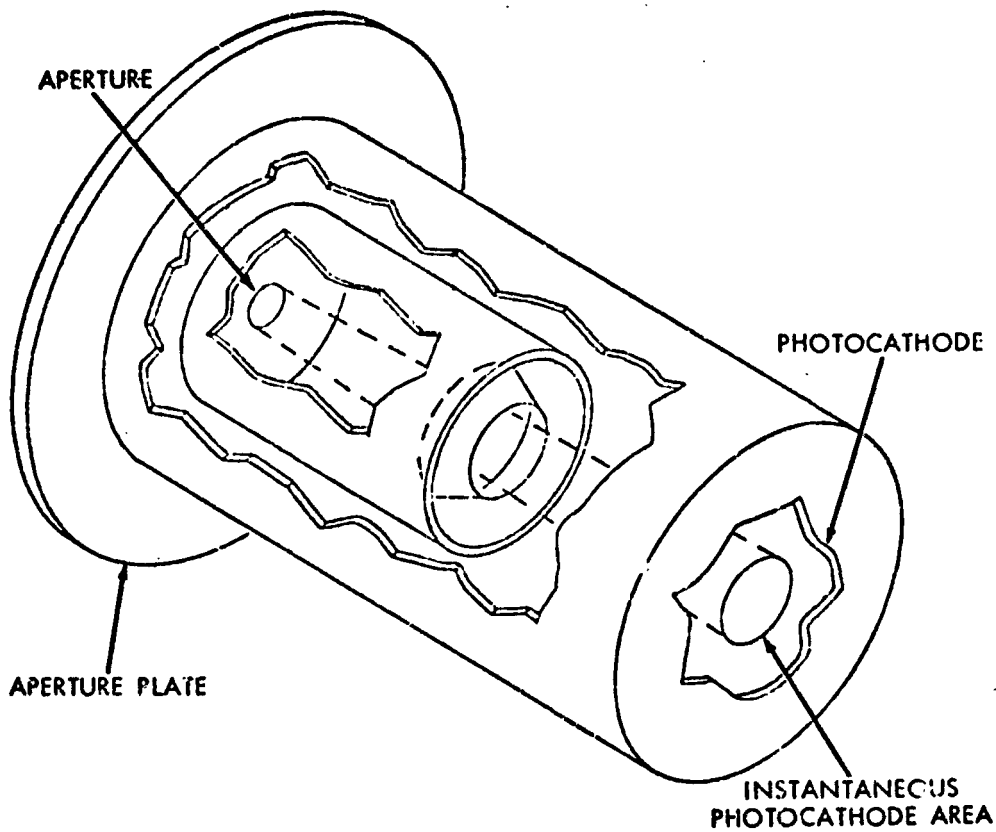

Figure 2-1. Image Dissector

current, the electron image can be swept across the limiting aperture. Mode control logic locks the tracker operation into the search mode at turn on. An acquisition field is generated by a 32 x 32 step raster scan with a step rate of 6.4 KHz and frame rate of 6.25 Hz. The acquisition field-of-view is approximately equal to 100 arcseconds. Acquisition stops when an image of the proper intensity and spectral content enters the instantaneous field-of-view and the tracking mode of operation is initiated.

In the tracking mode, a 400 Hz cross scan sweep causing pulse position and pulse duration modulation of the electron beam is employed as in Figure 2-2. The cross scan pattern is generated by deflecting the square instantaneous field-of-view from position "1" to form the pattern shown. The X-Y deflection voltage required to generate the pattern are also shown in Figure 2-2. A point source

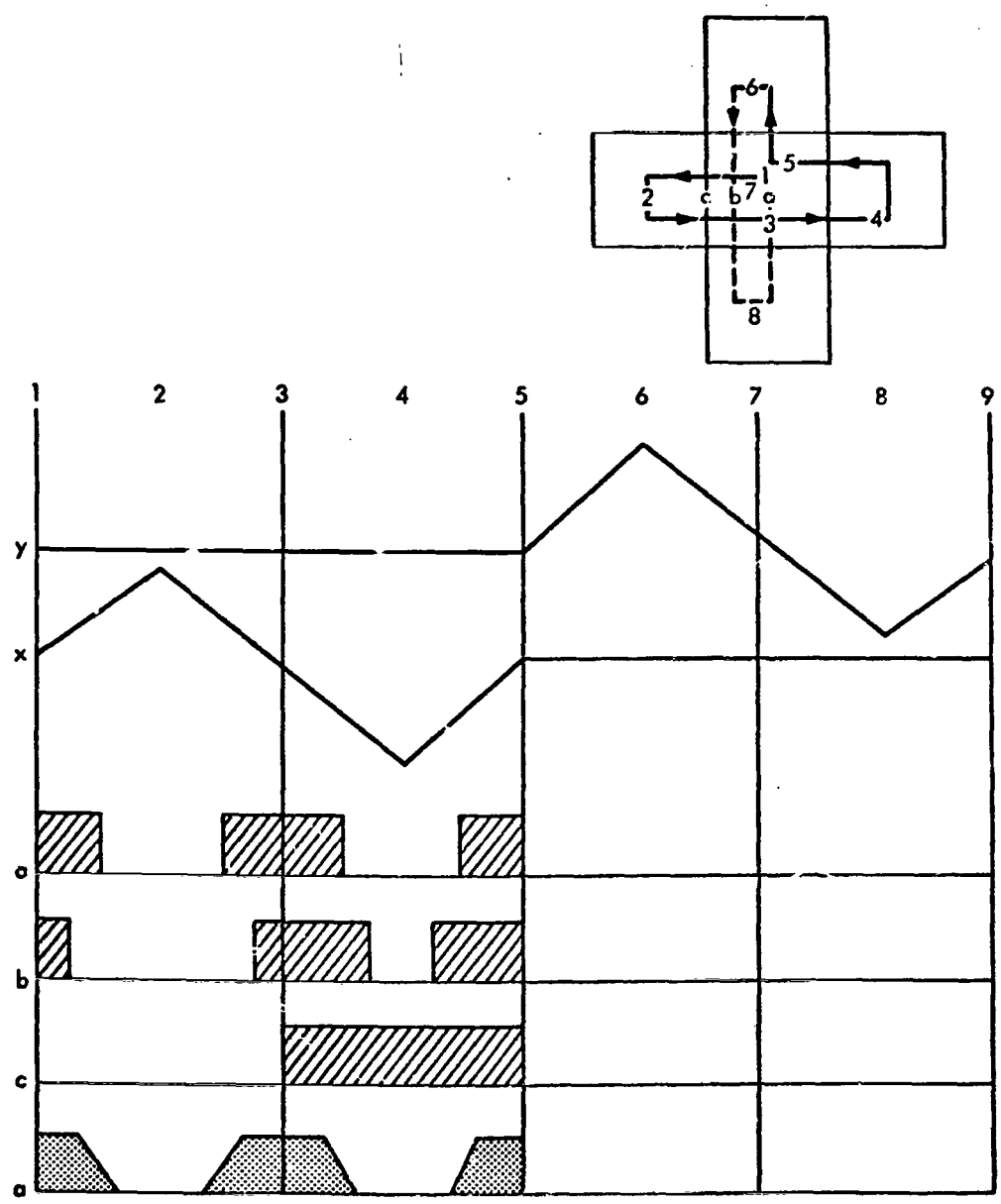

Figure 2-2. Target Signal Characteristics (Track Mode)

target at various central positions (a, b, & c) and the resulting video signals are shown in the diagram. When the target is in position "a", the integral of the output signal between "1" and "3" is equal to that between "3" and "5". The X axis error signal, which is the difference between these two areas, after processing, is zero. Clearly the Y axis error is generated in a similar manner from the remaining portion of the cross pattern "5" to "1". One example of an extended target is shown to illustrate that the operation and accuracy of the tracker is not limited to point source targets. Demodulator circuits develop the analog error which is used to control the DC deflection coil currents such that the cross scan is centered on the target image. These error signals are used in an internal closed-loop control system to follow the target image across the photocathode by electronically off-setting the electro-optical axis of the tracker. The current flowing through the deflection coil consists of a DC component which is proportional to the angle between the optical axis of the sensor and the target line of sight, and an AC component due to the track sweep waveform. The coil current is monitored through a low-pass filter to recover only the DC component which is then used to drive the tracker mount. A block diagram of the electro-optical tracker is shown in Figure 2-3. Tracking error was experimentally determined to be between 0.6 and 3.0 arcseconds rms depending on time of day and turbulence. The system has a maximum double lockup range of about 32 Kilometers by design. Furthermore, effective system lockup is limited to elevation angles greater than 20 degrees due to the fact that the tripod "feet", which support the flight package on the ground, can block the Argon beam as they swing relative to the cylindrical cannister containing the startracker. The cannister is, of course, locked in a specific orientation with respect to the ground station when the system is in autotrack. A photograph of the total ground station is given in Figure 2-4.

2.2 Ground Station Receiver

2.2.1 General Description

The ground station receiver for the heterodyne link was designed to utilize an intermediate frequency of 20 MHz. The entire receiver was mounted to a 76 cm by 76 cm aluminum plate which was, in turn, bolted to the trunnion of the main scope. The CO_2 radiation from the transmitter was collected by the 76 cm diameter telescope described previously and was reflected from a dichroic beam splitter placed directly in front of the startracker lens. The reflected radiation passed by means of a light pipe through an aperture in the bottom of the receiver mounting plate where it was again reflected by Mirror M1 (see Figure 2-5) resulting in a beam parallel to the receiver plate. The transmitter beam was focused on the mixer through beam splitter B2 by the Irtran lens L having a focal length of 13 cms. An Irtran lens was used due to its ability to pass visible and infrared radiation which made optical alignment much simpler.

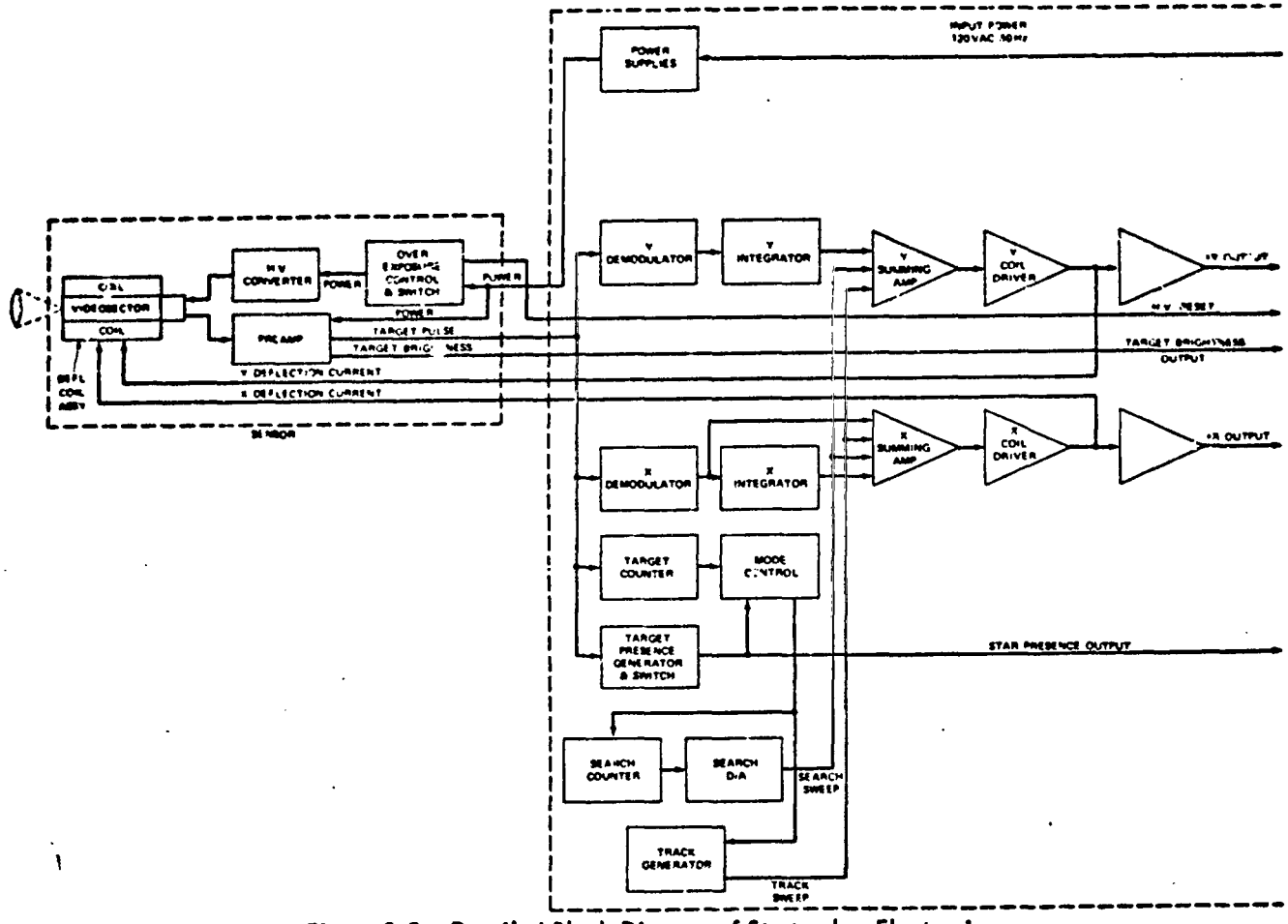

Figure 2-3. Detailed Block Diagram of Startracker Electronics

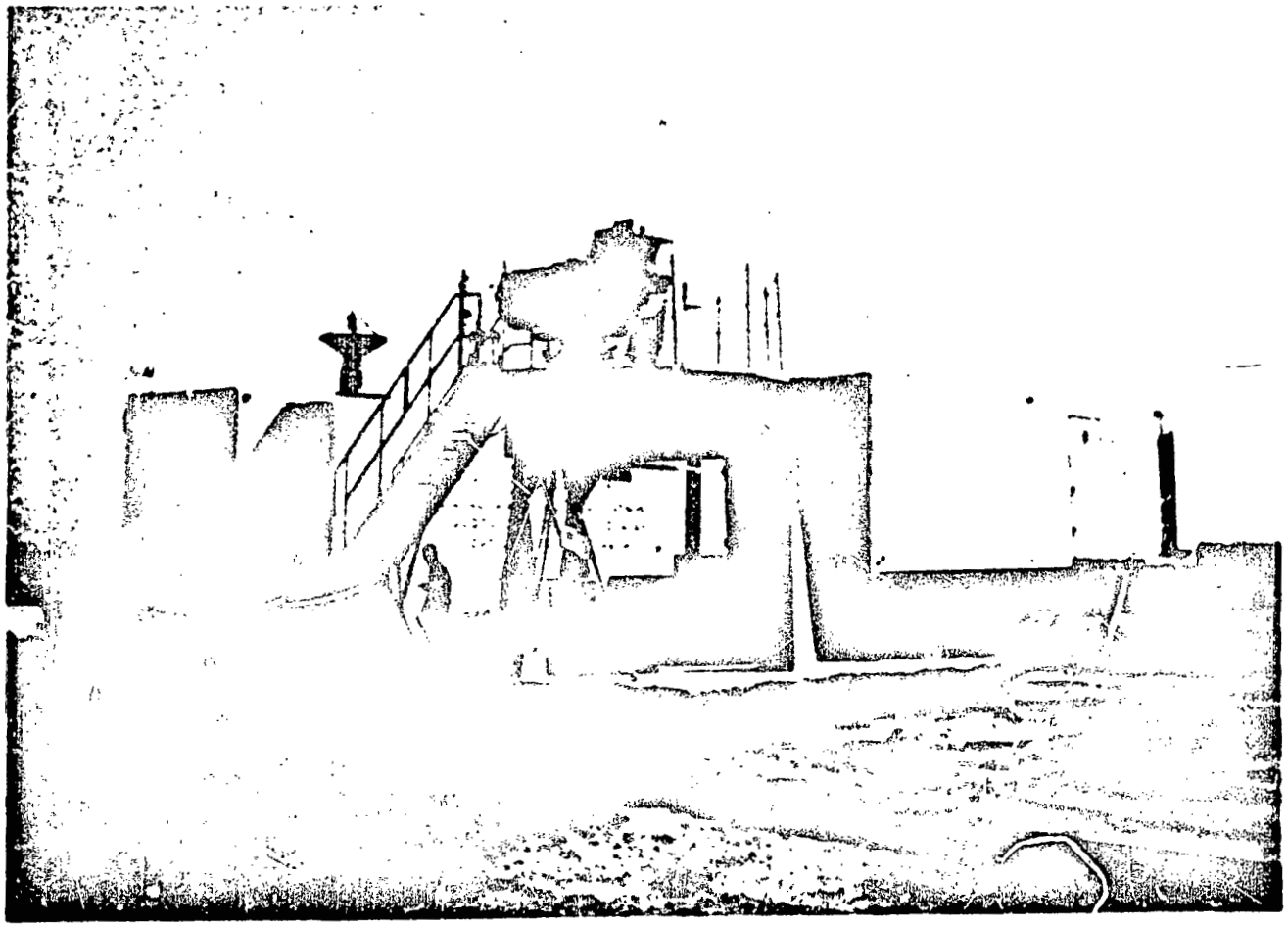

Figure 2-4. Total System

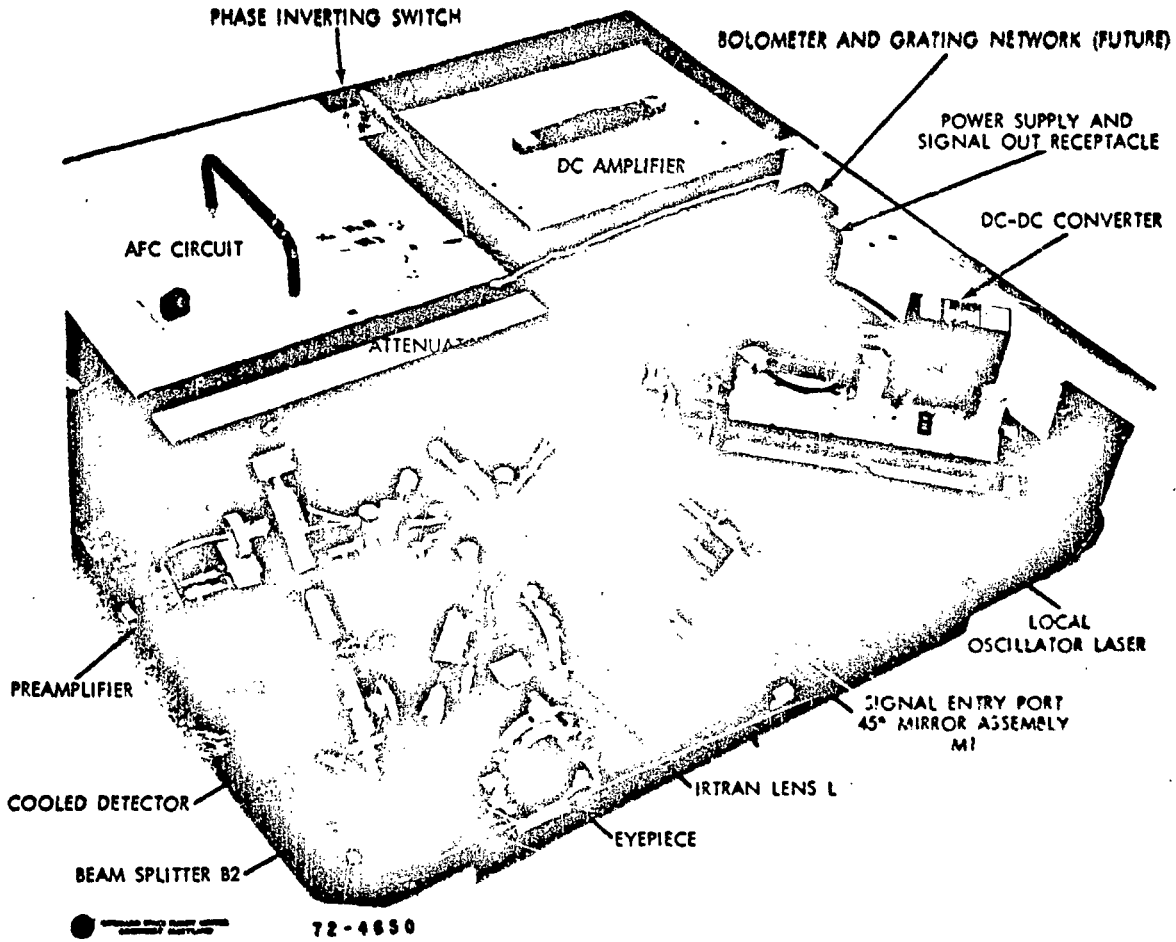
PHASE INVERTING SWITCH
BOLOMETER AND GRATING NETWORK (FUTURE)
POWER SUPPLY AND SIGNAL OUT RECEPTACLE
DC AMPLIFIER
DC-DC CONVERTER
AFC CIRCUIT
ATTENUATOR
LOCAL OSCILLATOR LASER
PREAMPLIFIER
SIGNAL ENTRY PORT 45° MIRROR ASSEMBLY M1
COOLED DETECTOR
IRTRAN LENS L
EYEPIECE
BEAM SPLITTER B2
72-4650

Figure 2-5.

The local oscillator laser, designed and built at Goddard Space Flight Center, was mounted on the receiver plate and powered by an Arnold Magnetics Corporation DC-DC converter which converted 28 VDC to a nominal 3500 VDC. Further details on the laser design and characteristics are given in Section 2.3.1.

The major portion (99%) of the local oscillator output power passes through the beam splitter B1 and is reflected off Mirrors M4 and M3, passes through attenuator A (typically 10% transmission), reflects off Mirror M2 and beam splitter B2 into the mixer port. The frequency of the local oscillator is manually controlled by applying a DC bias voltage from the Lansing DC amplifier to the local oscillator PZT. (Beam splitter B1 was originally included in the ground station design so that laser oscillation on the P(20) molecular line could be monitored by a grating and bolometer network which, unfortunately, was not available in time for the experiment.)

The combined transmitter and local oscillator signal at the mixer output is filtered and amplified and fed to the input of a discriminator which generates a voltage output proportional to the difference between the intermediate frequency (IF) and the nominal 20 MHz center frequency of the discriminator (provided the intermediate frequency is within the discriminator bandwidth). The intermediate frequency is, of course, the difference between the transmitter and local oscillator frequencies (see Appendix A).

The signal is then passed through a unity gain circuit which can either pass the signal unchanged or invert it. The latter is included in case the voltage generated by the discriminator is of the wrong polarity for LO tracking of the transmitter laser. The signal then enters a variable gain input of the Lansing DC amplifier which amplifies the incoming signal and superimposes it onto the DC bias supplied to the local oscillator PZT thus completing the feedback loop. The frequency of the local oscillator is now offset from the transmitter frequency by 20 MHz determined, of course, by the center frequency of the discriminator (the frequency input to the discriminator which gives zero output voltage).

2.2.2 Mixer Characteristics

The mixer employed in this experiment was a liquid nitrogen cooled mercury-cadmium-telluride (HgCdTe) SAT photodiode biased at 200 millivolts and having an area of 0.16 mm^2. The I-V characteristics with and without laser illumination are shown in Figure 2-6. Other mixer test data is given in Table 2-1 where it may be noted that the noise equivalent power for the device is experimentally found to be 2.2×10^{-13} W/Hz, representing an almost quantum-limited detection capability.

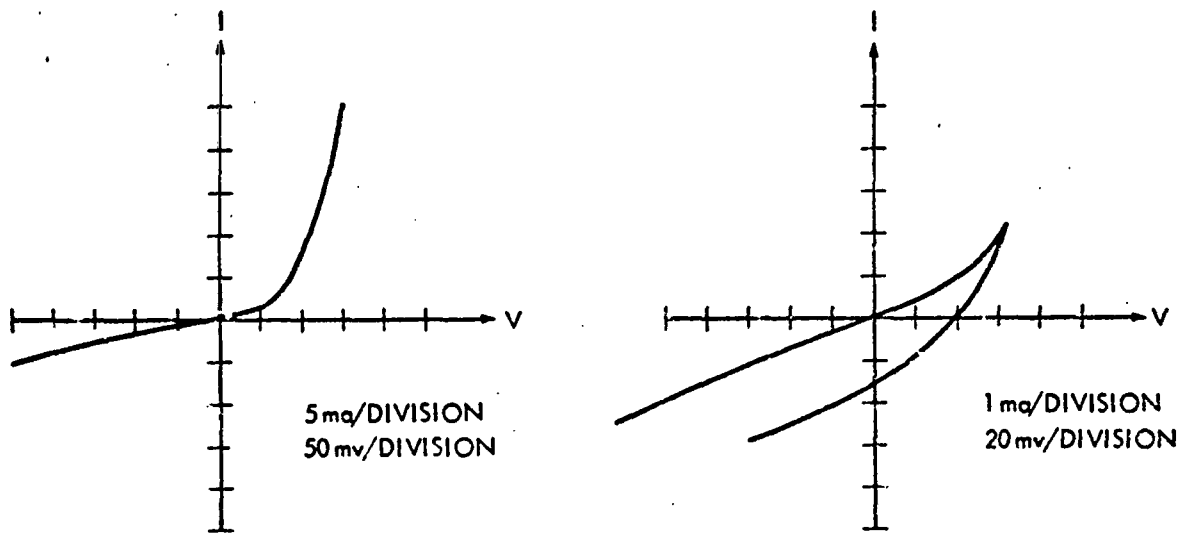

Figure 2-6. Detector Characteristics

Table 2-1

Mixer Test Data

Bias Conditions	
Voltage	200 mv
I dark	4.09 ma
I total	6.09 ma
I o	2.0 ma
Noise Equivalent Power Measurement	
Frequency	200 MHz
Power Input	2.77×10^{-8} watts
Mixed Signal	53.7 db
Noise, N	5.7 db
S/N	48.0 db
S/N Ratio	6.3×10^{4}
Noise Bandwidth	2×10^{6} Hz
NEP	2.2×10^{-19} W/Hz

2.2.3 Characteristics of the Receiver Electronics

The frequency bandpass and voltage output characteristics of the ground station receiver frequency-locking electronics are given in Figures 2-7 (a-k) and Table 2-2. The ground station was designed so that one of two alternate electronic systems could be chosen at will. The first system, designed and built by AIL, is described by Figure 2-7 and is the more sophisticated of the two. The Lansing DC Amplifier was not part of the AIL package but was included to fulfill a need for a variable DC bias source and a means of amplifying the AFC output and applying it to the local oscillator PZT. The second system

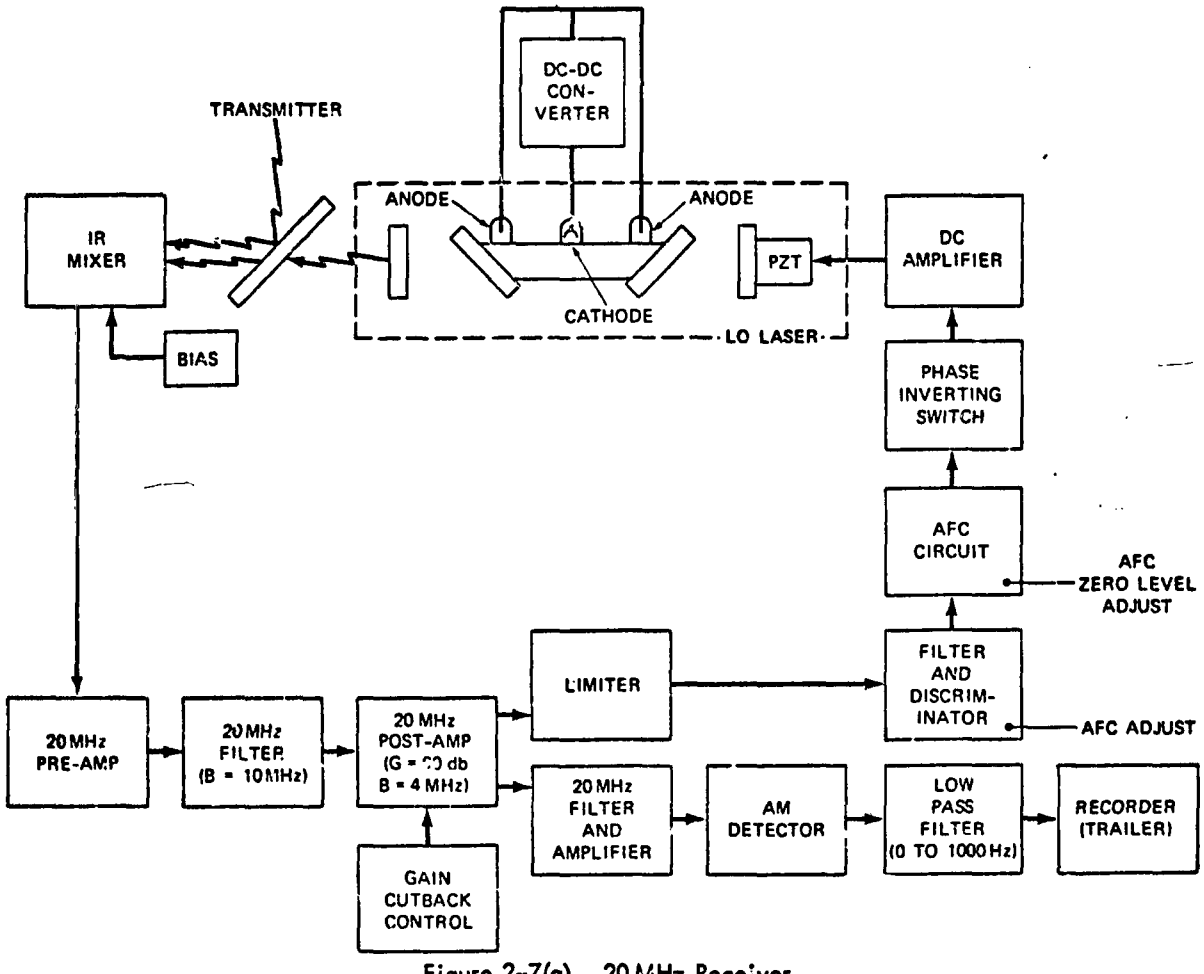

Figure 2-7(a). 20 MHz Receiver

PREAMP

GAIN = 29 db

BW_3 = (3-51.2) 48.2 MHz

BW_1 = (9-47.2) 38.2 MHz

N.F. = 2 db

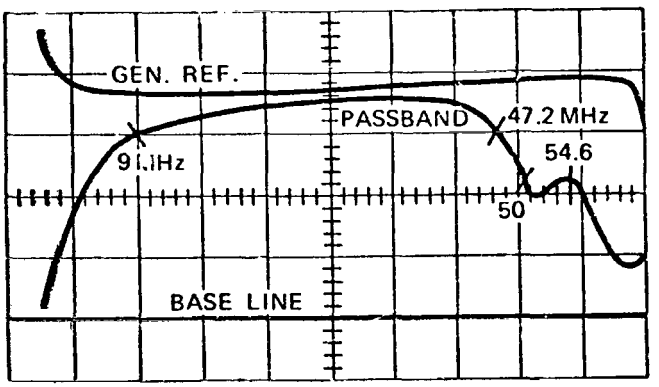

SCOPE SENSITIVITY
VERT 0.5 mv/cm
HORIZ 0.5 v/cm

Figure 2-7(b)

NOISE BANDWIDTH FILTER

IL = 0.5 db

BW_3 = (14.3-26.8) 12.5 MHz

BW_1 = (14.8-26) 11.2 MHz

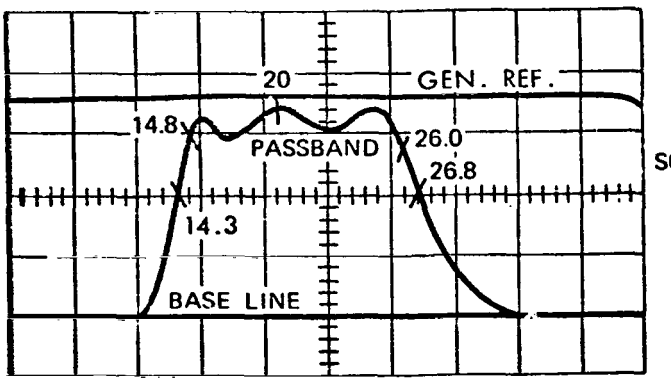

SCOPE SENSITIVITY
VERT 0.2 mv/cm
HORIZ 0.5 v/cm

Figure 2-7(c)

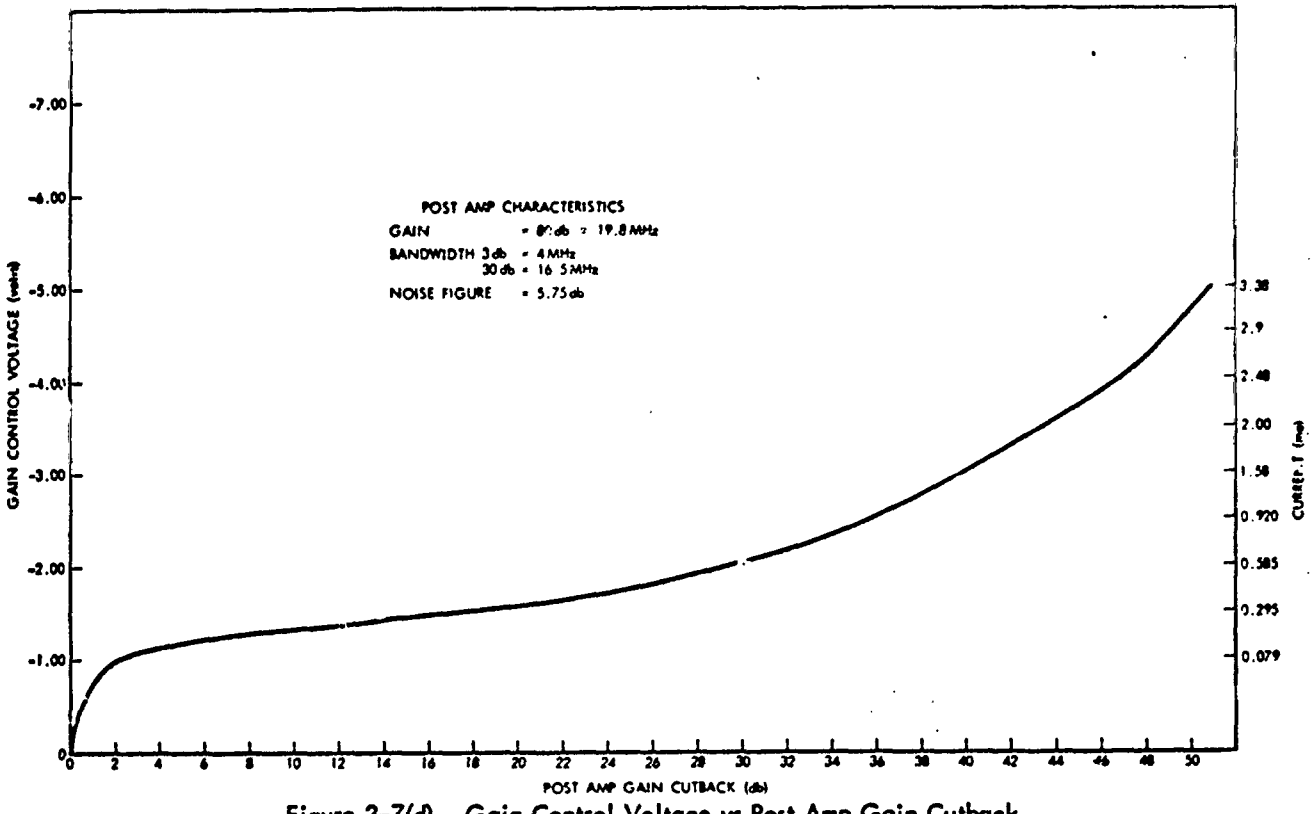

Figure 2-7(d). Gain Control Voltage vs Post Amp Gain Cutback

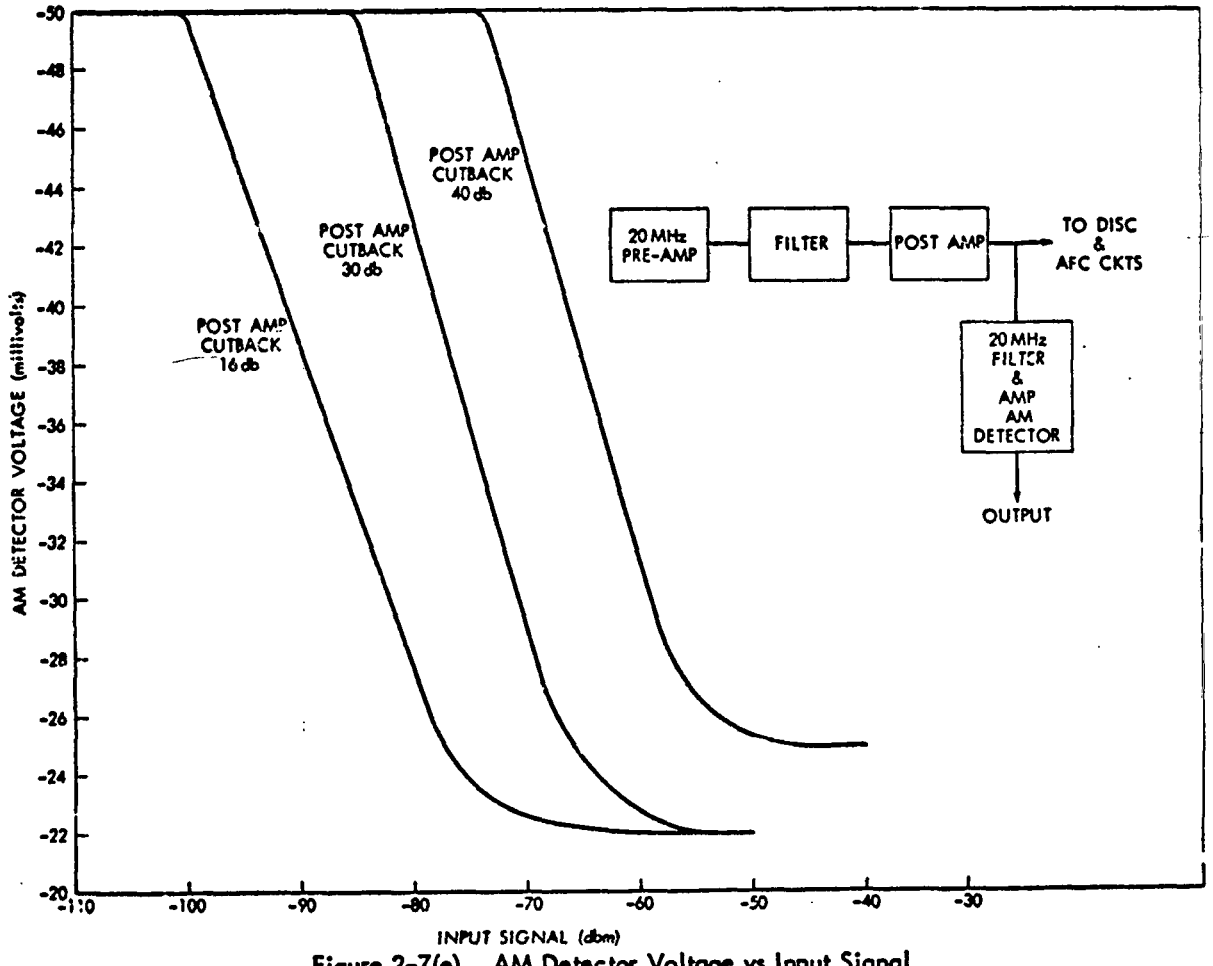

Figure 2-7(e). AM Detector Voltage vs Input Signal

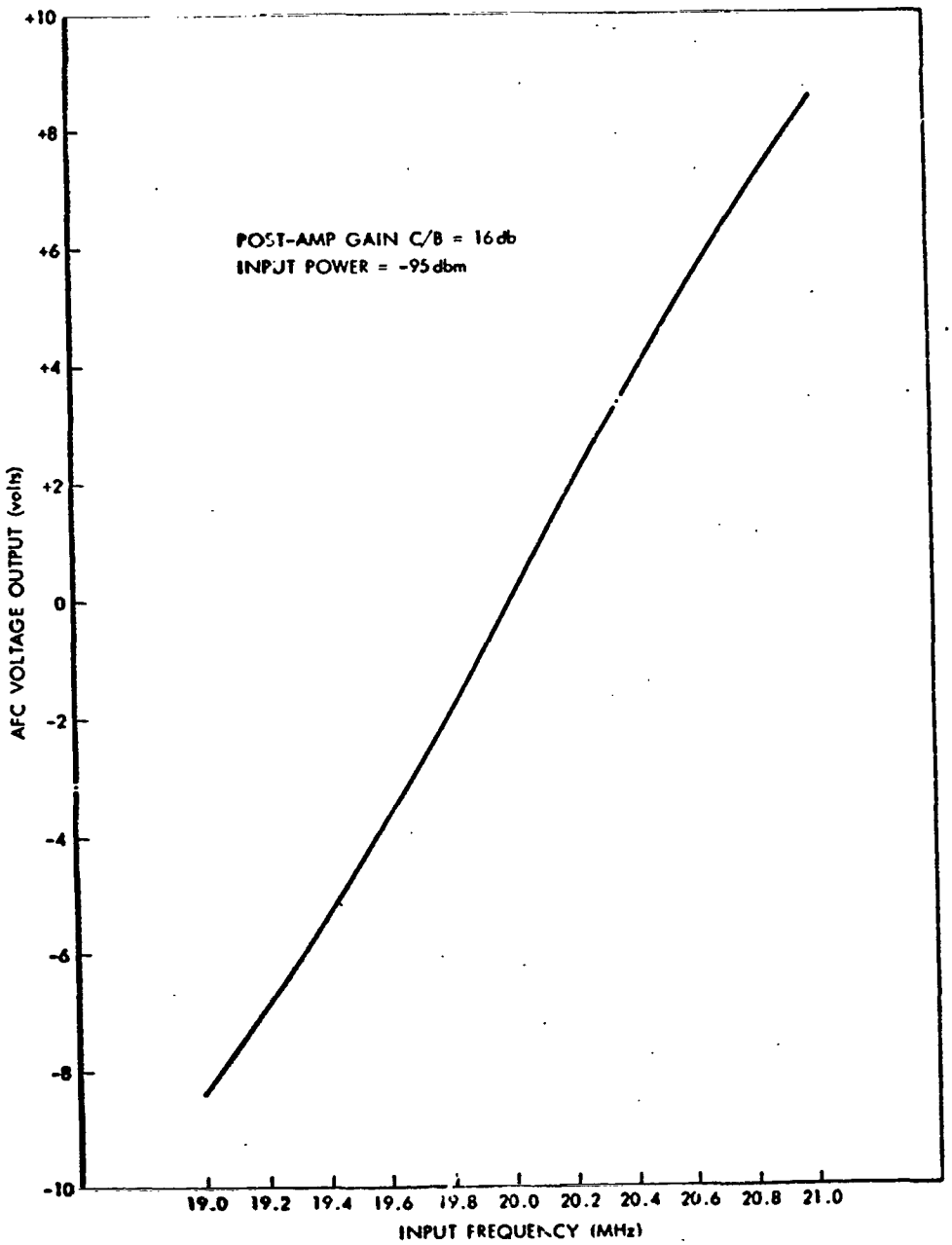

Figure 2-7(f). AFC Voltage Output vs Input Frequency

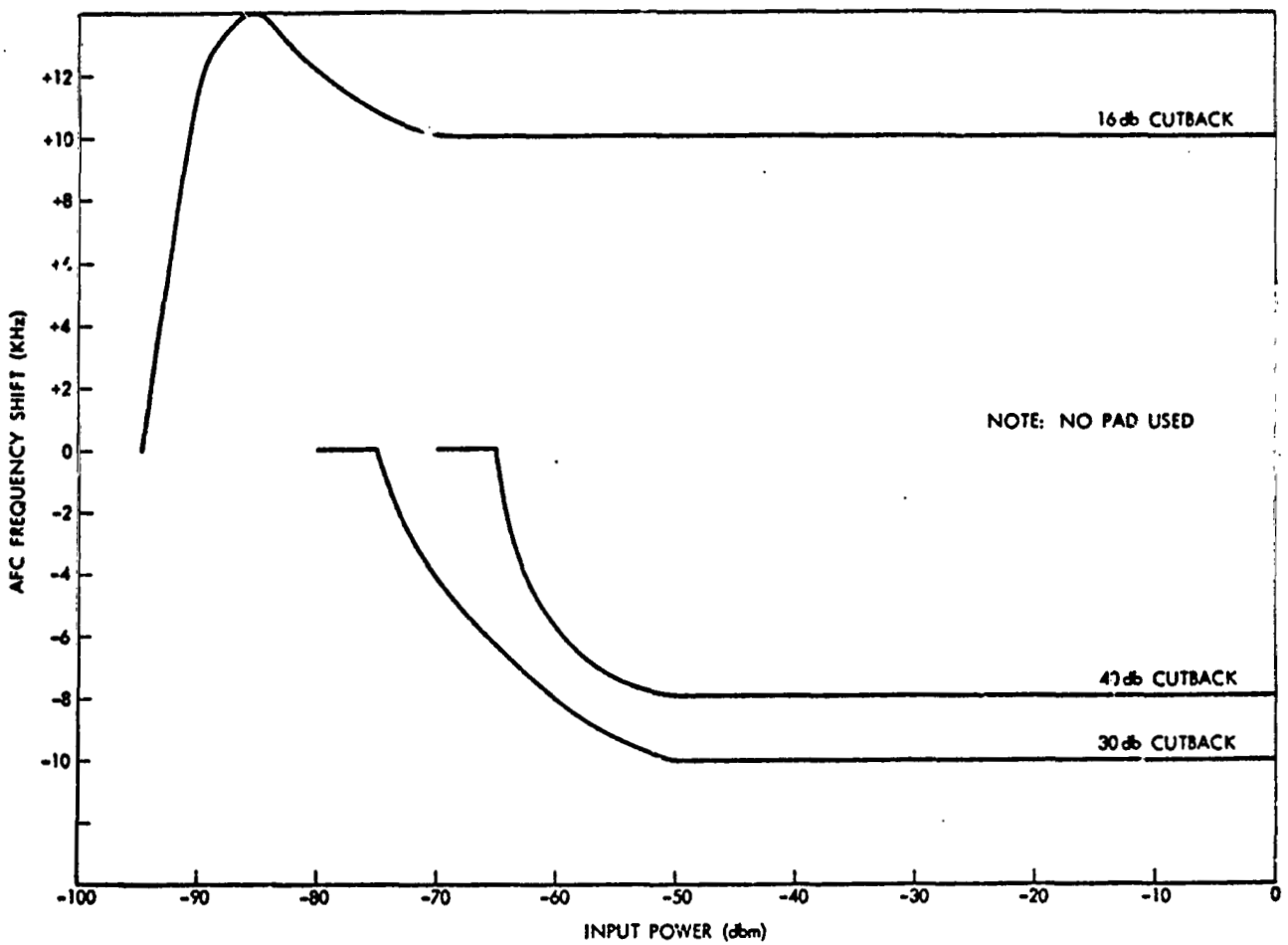

Figure 2-7(g). AFC Frequency Shift vs Input Power With Post-Amp Gain Cutback as a Parameter

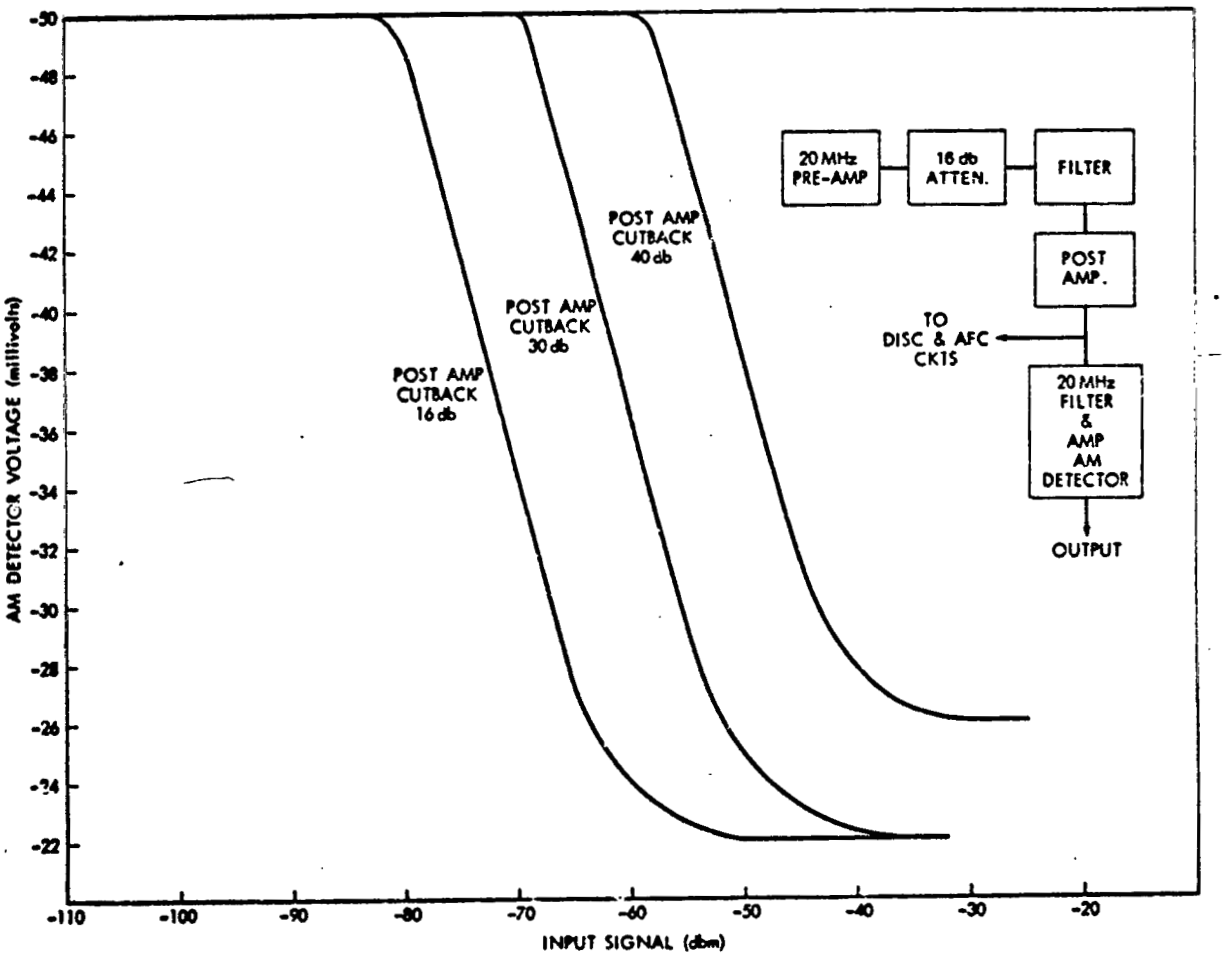

Figure 2-7(h). AM Detector Voltage vs Input Signal

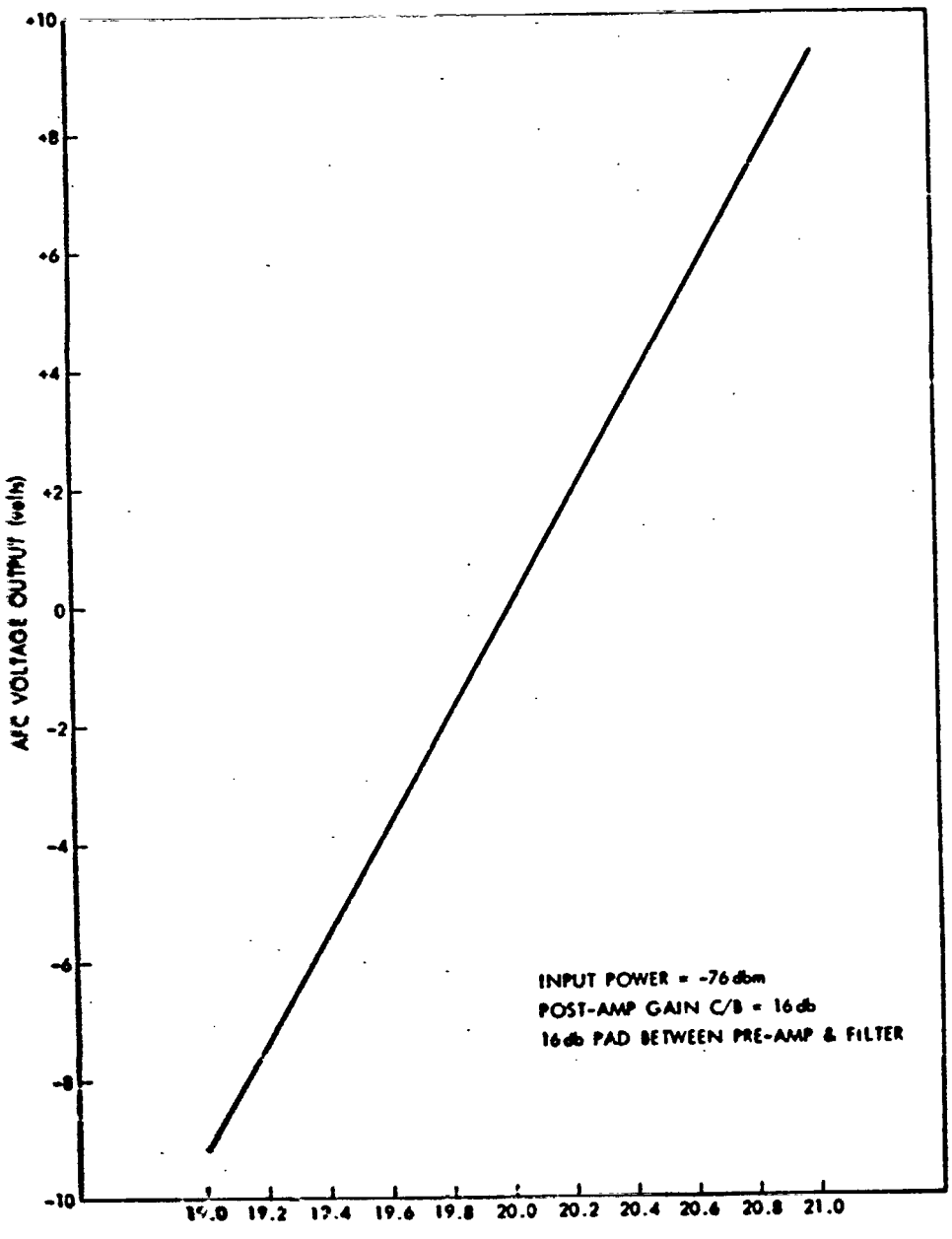

Figure 2-7(i). AFC Voltage Output vs Input Frequency

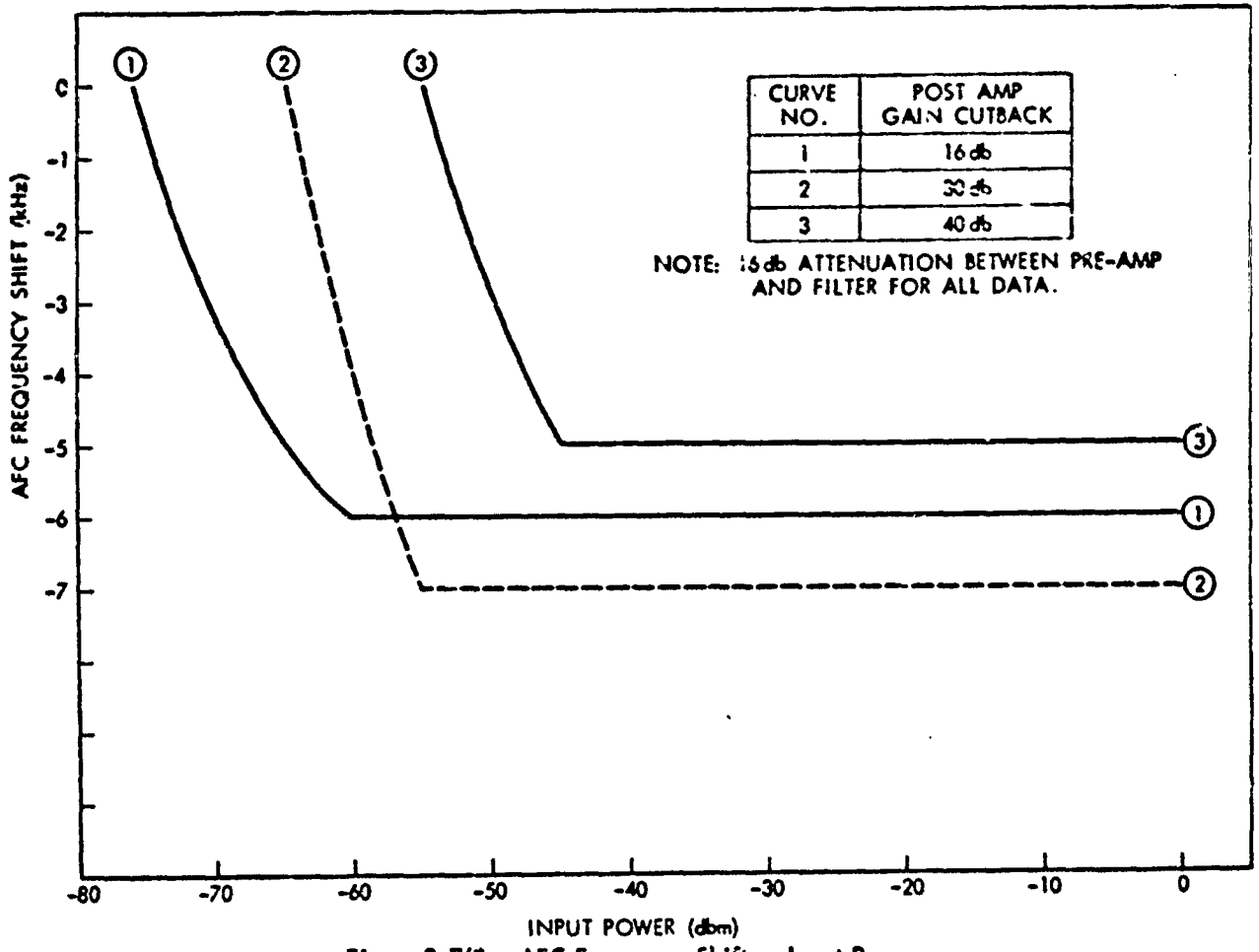

Figure 2-7(j). AFC Frequency Shift vs Input Power

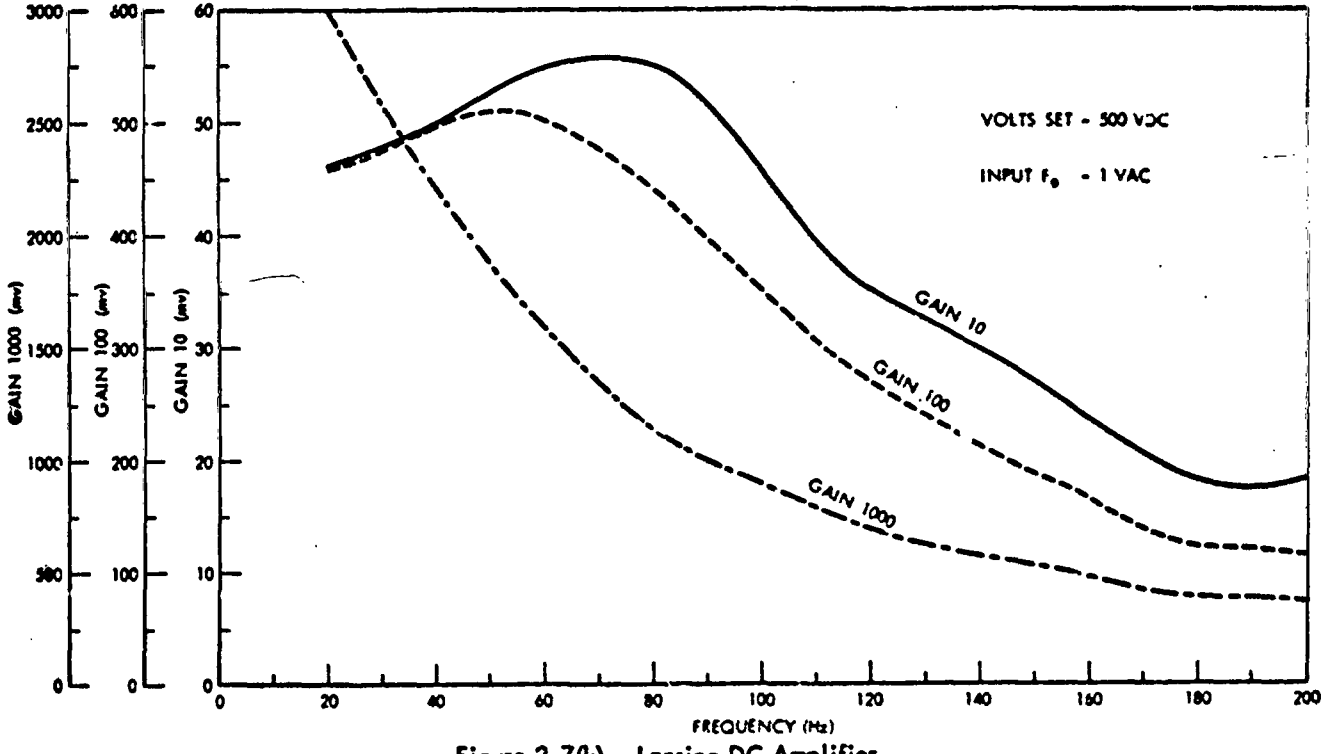

Figure 2-7(k). Lansing DC Amplifier

Table 2-2

Characteristics of RHG IF Amplifier and Discriminator

RHG IF Amplifier Model EVT2004	
Center Frequency:	20 MHz
3 db Bandwidth:	4 MHz
Noise Figure:	2.8 db
Maximum Power Gain:	81 db
Maximum Voltage Gain:	101 db
Power Output:	+19.6 dbm
Maximum Voltage Output:	8.5 V/93 Ω
Gain Control Range:	50 db at -3.9 VDC
Current Drain:	+12 VDC at 100 ma
RHG Discriminator Model DT2004	
Center Frequency:	20 MHz
Peak to Peak Bandwidth:	6 MHz
Video Output Sensitivity:	Set at 1 V/MHz
DC Output Sensitivity:	205 MV/MHz
Risetime:	0.25 μsec
Linearity:	> 5% over ±2 MHz
Power Drain:	+12 VDC at 40 ma -12 VDC at 40 ma

utilized the AIL preamplifier and the Lansing DC Amplifier but replaced all of the intermediate components by an RHG 20 MHz amplifier and discriminator whose characteristics are described in Table 2-2.

2.3 Flight Package

2.3.1 CO_2 Laser Transmitter

The CO_2 lasers used as the airborne transmitter and the ground station local oscillator in the present experiment are of a Goddard Space Flight Center design. The laser is shown as part of the flight package in Figure 2-8 (a). The tube is designed to survive the Titan III C launch environment and be passively cooled (i.e., no circulating coolants). The approach that was taken to satisfy both these requirements was to pot the tube into an aluminum heat sink using Solithane 113 (Thiokol Chemical Corporation) as the potting material. This is a versatile polyurethane potting compound whose formulation can be varied to provide a wide range of Shore "A" hardness values. It is widely used in the potting of spacecraft components because of its low outgassing characteristic.

During potting, the tube is centered in the heat sink with teflon rings. The heat sink is designed to provide a uniform 1.6 mm thickness of potting material between the plasma region of the main bore of the tube and the sink. This thickness varies in less critical areas. The Shore "A" hardness value of the material used in potting these tubes was between 75 and 80.

The tube is made of Pyrex and consists of a main bore of 5.5 mm diameter which has a 30.5 cm overall length. It has a central cathode made of nickel and two tungsten pin anodes that provide a discharge length of 20.3 cm. Located on either side of the main bore and interconnected to it through a glass tee are two gas reservoirs. These provide a total gas volume of 75 cc. The tube is equipped with GaAs Brewster windows.

The optical cavity of the laser consists of an invar yoke that mounts around the heat sink. One end of the yoke is mounted firmly to the baseplate while the other end is mounted with clips to permit the independent thermal expansion of the invar yoke and aluminum baseplate.

A dielectric coated germanium mirror with 95% reflectance on the inner surface and an AR coating on the outer surface is used on the output end of the laser cavity. The rear mirror is 7 mm in diameter and is mounted on the center of a double-disc bender Piezoelectric transducer. It has a 0.75 meter radius of curvature and is 100% gold coated. The PZT provides a tuning range of slightly more than 10 micrometers. Output power of the laser is approximately 0.75 watts in the TEM_{00q} mode.

The laser and control electronics were mounted on an aluminum baseplate and inserted into a hermetically sealed cannister as shown in Figures 2-8(a) through 2-8(d). The cannister in turn was positioned inside a cylindrical tube on the balloon flight package which also contained the airborne startracker. The direction of the transmitter beam was controlled by azimuthal and elevation servo systems which were in turn driven by startracker error outputs when the system was in autotrack.

2.3.2 Laser Control Electronics

The function of the laser control electronics is to produce a scan of the laser's operating frequency until the desired frequency is obtained; in this case, this corresponds to obtaining operation on the P(20) line of the laser, at a center frequency of 28,306,251 MHz. After operation on the proper line is secured, which tunes the laser to within nominally ±50 MHz of the final desired operating frequency, the laser control electronics must generate appropriate signals to cause the laser to seek and remain at the peak of the operating line, which also corresponds to the center frequency of the line.

Figure 2-9 shows a block diagram of the laser control electronics. Operation is initiated by telemetry command from the ground. With no power from the power detector, the output from the threshold circuit is a NOT THRESHOLD which throws the FET Switch (shown schematically as a block with two inputs) to connect the search oscillator into the integrator. The search oscillator has a 0.5 Hz square-wave output which becomes a triangular wave when passed through the integrator. The triangular wave is amplified in the tuner driver and applied to the piezoelectric bender bimorph. When the cavity is tuned to the proper wavelength (the cavity length is adjusted by the bender bimorph), the power detector delivers a voltage which triggers the threshold circuit. This action throws the FET switch into position for dither stabilization.

The dither oscillator is operating at 75 Hz and is fed to the input of the tuner driver; this produces a frequency modulation of the laser at the dither frequency. Because of the shape of the laser's gain curve, shown in Figure 2-10, the frequency modulation is accompanied by amplitude modulation at the bolometer at twice the dither frequency when the laser is centered on the line. If the laser is operating to either side of the line center, the laser is amplitude modulated at the dither frequency but with differing phase. This is also depicted in Figure 2-10. By detecting the amplitude modulation in synchronism with the dither frequency, a discriminator-like curve is generated that has a zero at line center. Thus, an error signal is generated that has a zero at line center, and the tuner is driven until the laser is operating at line center.

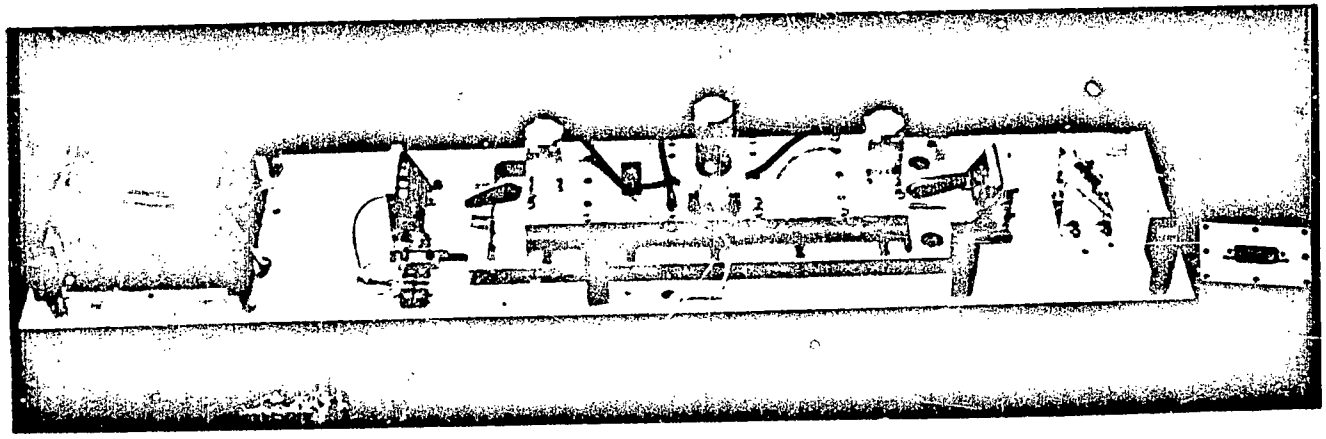

Figure 2-8(a)

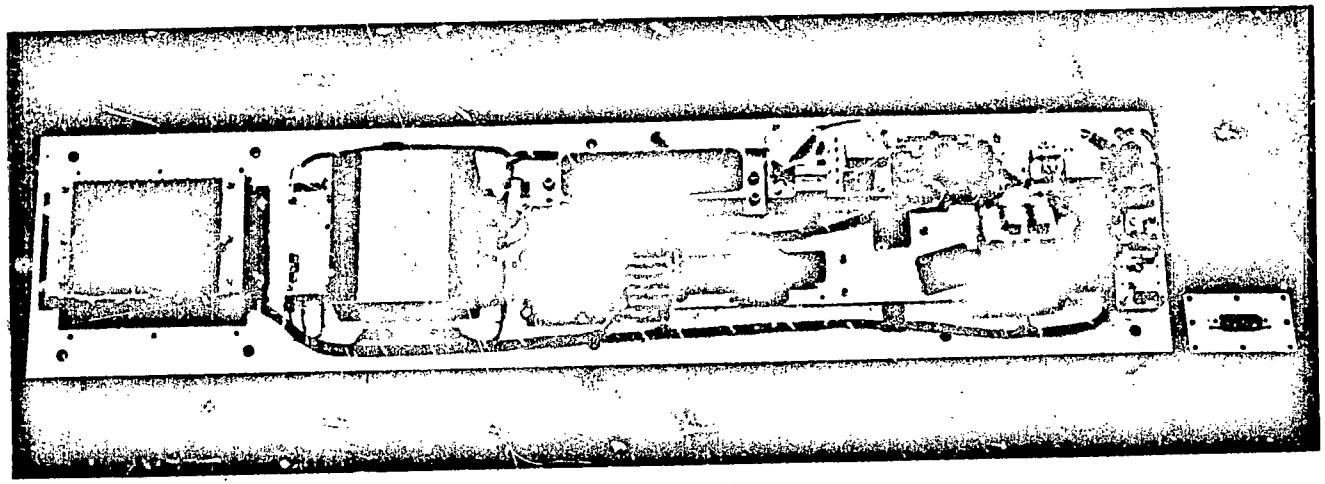

Figure 2-8(b)

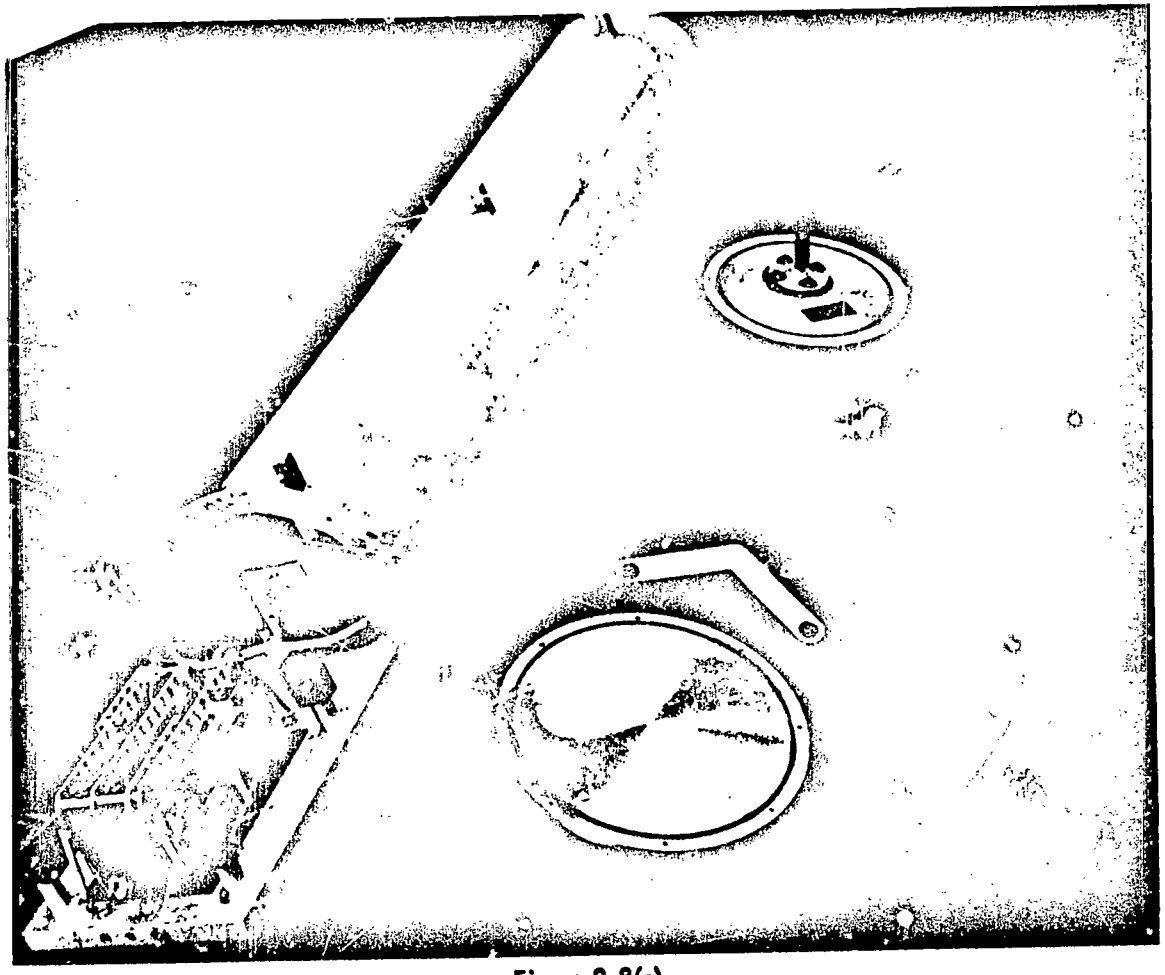

Figure 2-8(c)

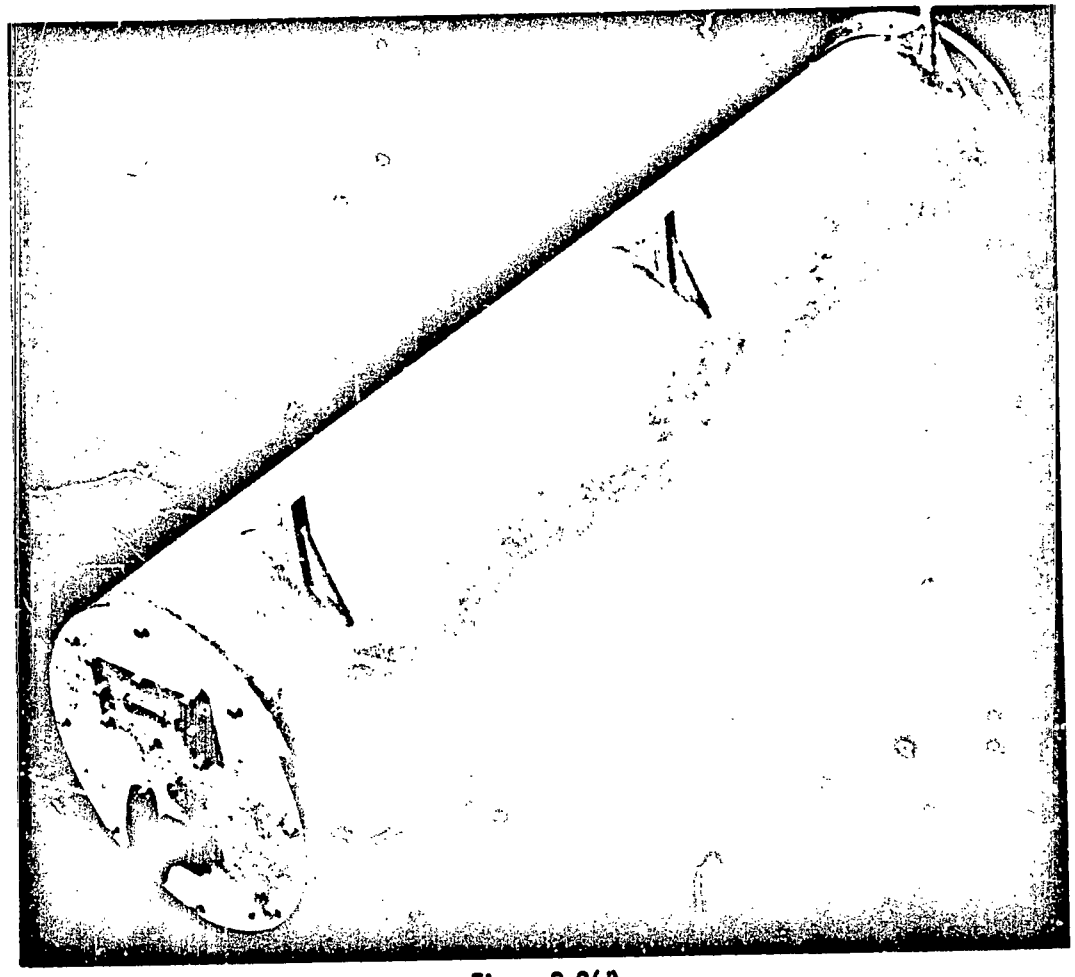

Figure 2-8(d)

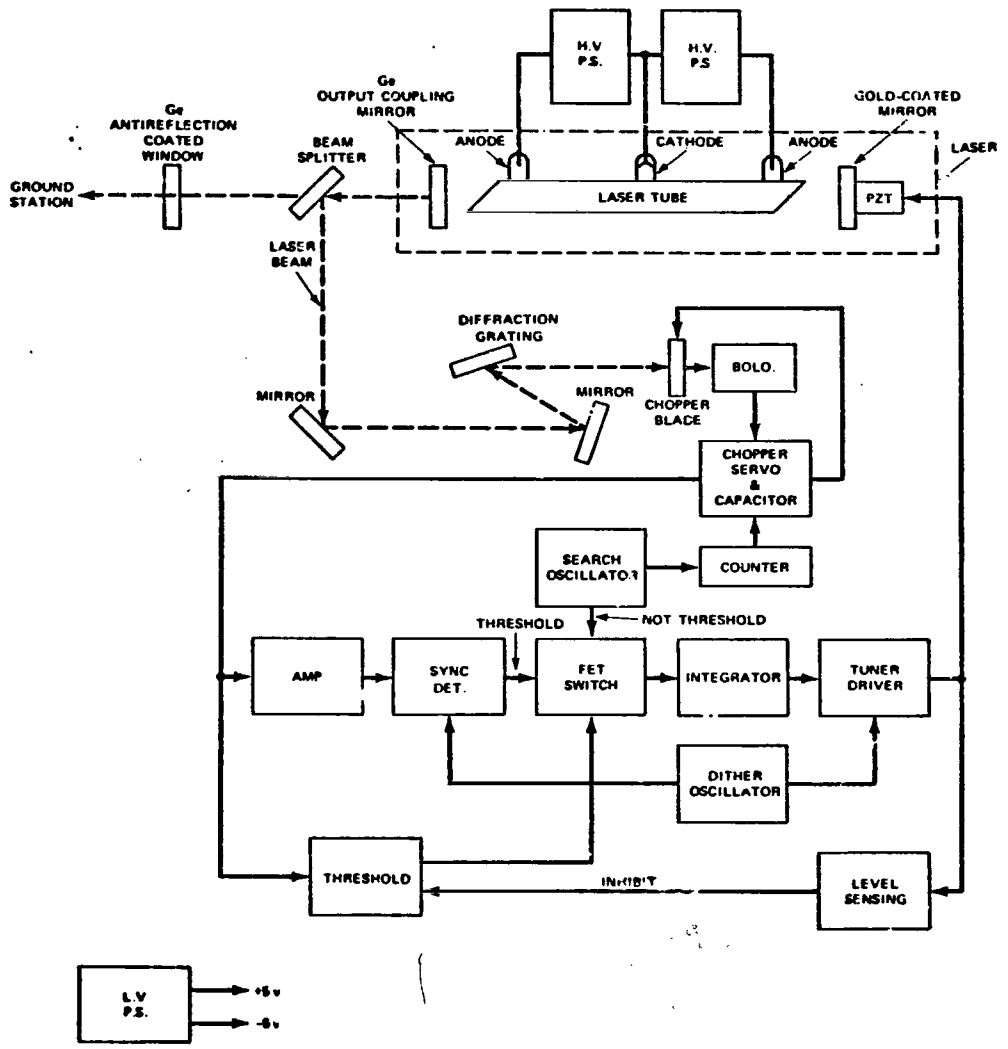

Figure 2-9. Laser Control Electronics

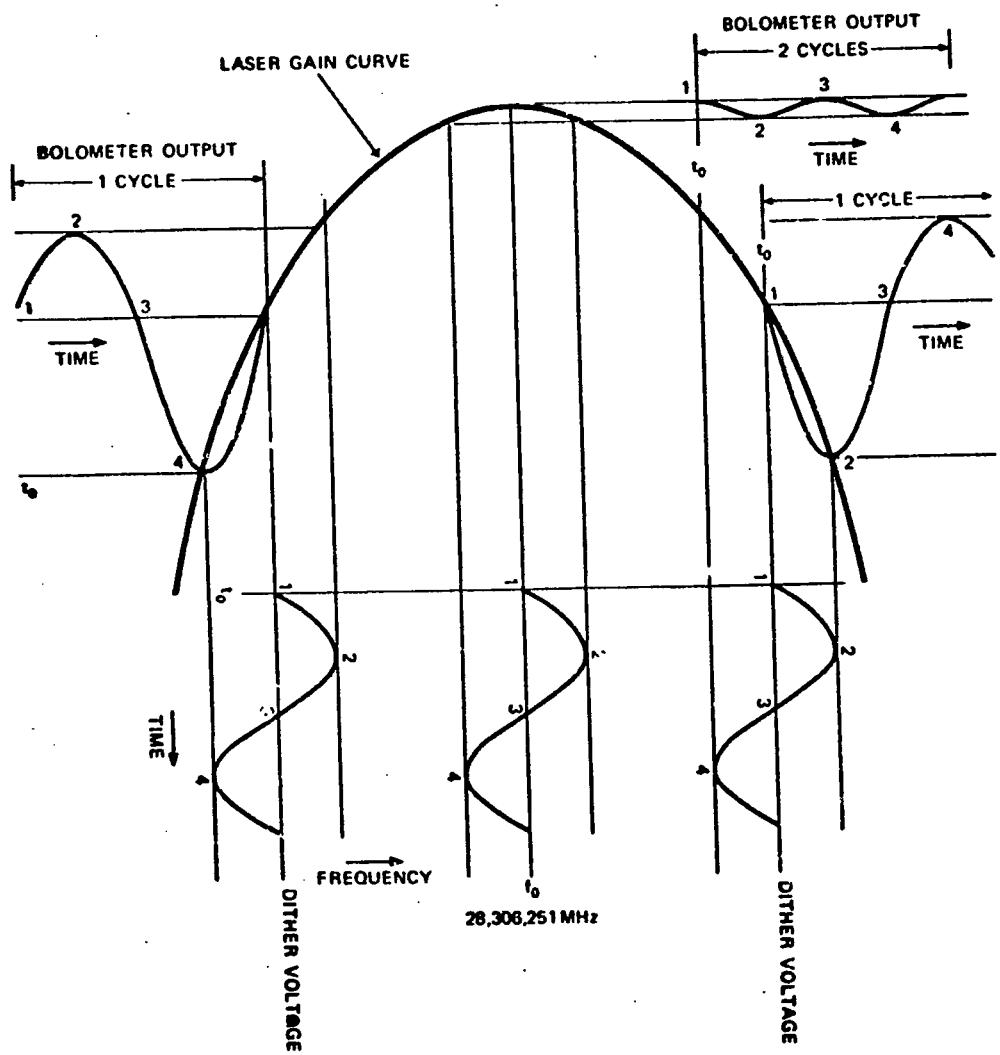

Figure 2-10. Dither Stabilization

A level sensing and inhibit circuit is included to prevent lock-on at either extreme of the range of the tuner driver and thereby prevent lock-on on partial profiles. The range of the ramp voltage is chosen so that the cavity length can be changed by an amount greater than one-half the wavelength of the P(20) line. This guarantees that the P(20) line will be found at some interior point well within the range of the tuner driver. A typical bolometer response, due to the imposition of the 0.5 Hz ramp voltage on the tuner driver, is shown in Figure 2-11.

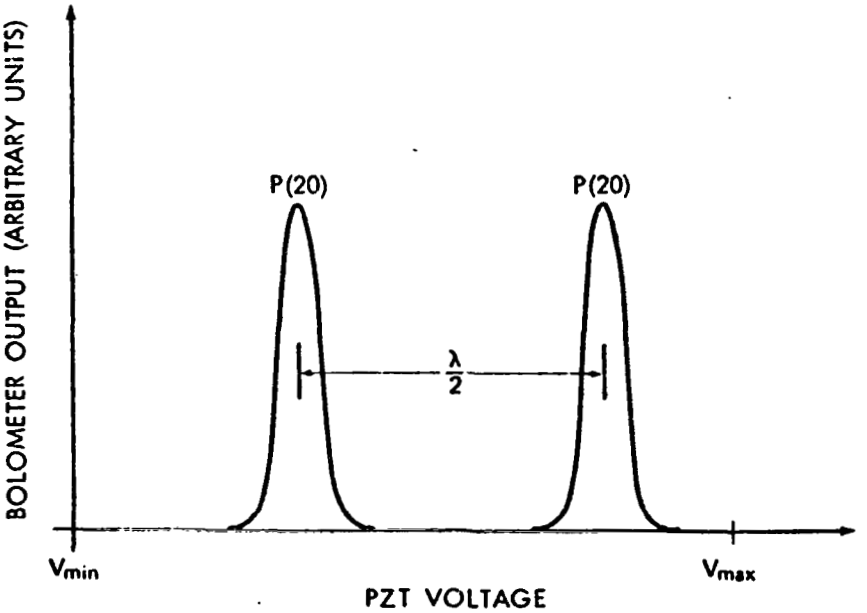

Figure 2-11

Because thermal variations between the active and compensator flakes in the bolometer image circuit occur over extended periods of operation, a spurious voltage is gradually built up at the output of the bolometer. This voltage eventually reaches a magnitude capable of triggering the FET switch giving a THRESHOLD reading even when the laser is not operating on the P(20) line. For this reason, it is necessary to cancel this voltage periodically. This is done in the following manner. A counter, made up of a series of flip-flop circuits, counts the square wave pulses generated by the 0.5 Hz oscillator. When (after a preset period of time) all of the flip-flop circuits are in the "on" mode, a voltage is generated at the output of the counter which causes a chopper to block the input to the bolometer. At that time the voltage which has been generated as a result of thermal drifts is fed to a high Q capacitor which applies the voltage

at one input to a differential amplifier thereby cancelling the thermal effect. The chopper blade then returns to its original position and the system again begins the search and dither operation described above. In the present experiment, the period between thermal resets was 256 seconds. At each reset, P(20) line operation was interrupted for 2 seconds.

3. PRE-FLIGHT ALIGNMENT PROCEDURES

3.1 Initial Alignment of Ground Station Receiver Optics

Because of the small detector size ($\sim 0.16\,mm^2$), the narrow field-of-view (~ 8 arcseconds) and the low signal levels ($\sim 10^{-6}$ watts) expected over the 1.2km horizontal range, it was advisable to carry out some sort of optical alignment procedure before mounting the ground station on the 76cm diameter scope. Mirror M1 (see Figure 2-5) was temporarily replaced by a mirror capable of accepting an incident beam parallel to the ground station baseplate. A helium-neon and a CO_2 laser were placed on a table next to the ground station as in Figure 3-1. The beam from the two milliwatt He-Ne laser was reflected from a dichroic beam splitter to a 30cm diameter flat approximately 34 meters away from the ground station receiver. To simplify the alignment procedure, the beam divergence was reduced by a passing the beam through a collimating telescope which allowed easy visual observation of the He-Ne spot at all points in the alignment network. The azimuthal and elevation tilt angles of the flat were adjusted so that the center of the beam fell on the aperture of the removable mirror at a height above the baseplate equal to the height of the local oscillator beam. The tilt angle of the removable mirror was then adjusted to pass the helium-neon beam through the center of the lens L.

The He-Ne and CO_2 transmitter beams were then made collinear by burning heat sensitive paper at two points along the He-Ne beam path. The separation distance between the two points was limited to about two feet due to the attenuation of the beam splitter and a fairly rapid CO_2 beam divergence. The use of small (~ 4 mm diameter) apertures at the two points aided in the alignment which was carried out by adjusting the CO_2 laser orientation.

The CO_2 signal was chopped at 450cps and the detector mount was adjusted for optimum signal. The signal was then maximized with respect to lens translation and focal point. The crosshairs on the eyepiece were centered on the helium-neon spot and the eyepiece travel adjusted for best focus and minimum parallax. The local oscillator beam was then centered on the detector by adjusting Mirror M2, after which the removable mirror was again replaced by Mirror M1. The ground station was then ready to be mounted on the 76cm diameter scope.

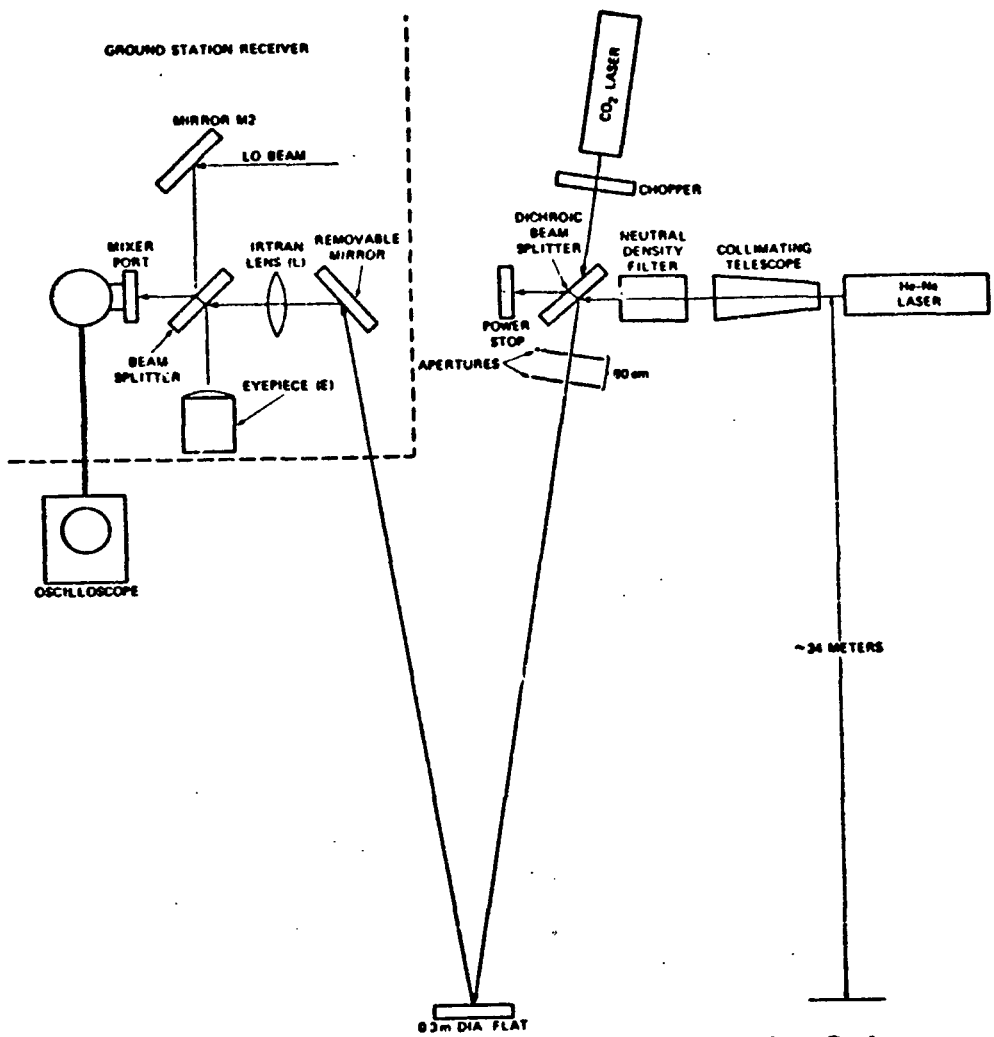

Figure 3-1. Initial Alignment of Ground Station Receiver Optics

3.2 Boresight Procedure for the Telescope, Lasers, and Coelostat Optics

A view of the total optical network used in the system boresighting procedure is given in Figure 3-2. The beam from a 4-watt Argon laser passes between the chopper blades, through a central aperture in Mirror A, and reflects off of the dichroic beam splitter. The purpose of the chopper (which is not used in the boresight procedure) is to provide a 5KHz modulation of the outgoing Argon beam to enable the flight package startracker to distinguish the laser beacon from the radiation background. Similarly, the CO_2 laser output is often chopped to assist in the final alignment of the ground station receiver described in the next section. During an actual heterodyne experiment, the CO_2 chopper is not used.

After passing through the chopper, the CO_2 beam enters a collimator where the beam divergence is reduced by a factor of 5 to allow greater signal return from the cube corner. Mirror C is oriented so that the Argon and CO_2 spots are superimposed at the dichroic beam splitter. Both beams (Argon and CO_2) travel on to Mirror B where they are reflected to Mirror D. Mirror D is indicated by dashed lines because it is only present during a portion of the boresight procedure. If Mirror D is in the position shown, the Argon and CO_2 beams are deflected to spherical Mirror E which focuses both beams onto heat sensitive paper taped on the screen. The tilt angle of the dichroic beam splitter is adjusted until the focused Argon spot and the CO_2 burn spot are superimposed (they are superimposed at infinity implying that the beams are parallel). Since they have already been superimposed at the dichroic beam splitter, the two beams are therefore collinear. The telescope "T" is adjusted so that the two focused spots fall on the instrument's crosshairs and Mirror D is removed. Mirror B is then adjusted so that the laser beams pass through the center of the light pipe leading from the trailer to the coelostat optics. The beams then travel out of the laser tube to the boresight target. If a heterodyne experiment off the cube corner is to be performed using the CO_2 laser in the trailer as the transmitter, the last coelostat mirror is tilted so that the cube corner on the target board 0.6 Kilometers away is centered on the crosshairs of the telescope inside the trailer since the telescope crosshairs indicate the direction of travel of the laser beams. On the other hand, if a boresight at infinity is desired, the last coelostat mirror is oriented so that the telescope crosshairs fall on the second target crosshair. The latter is displaced from the cube corner by an amount equal to the distance between the center of the receiving aperture of the main scope and the center of the laser tube bore. Similarly, the trackerscope, which is used by the tracking mount operator to bring the target within the acquisition field-of-view of the startracker, is focused on the first target crosshair which is displaced from the cube corner by an amount equal to the distance between the centers of the receiving apertures for the tracker and main scopes. During

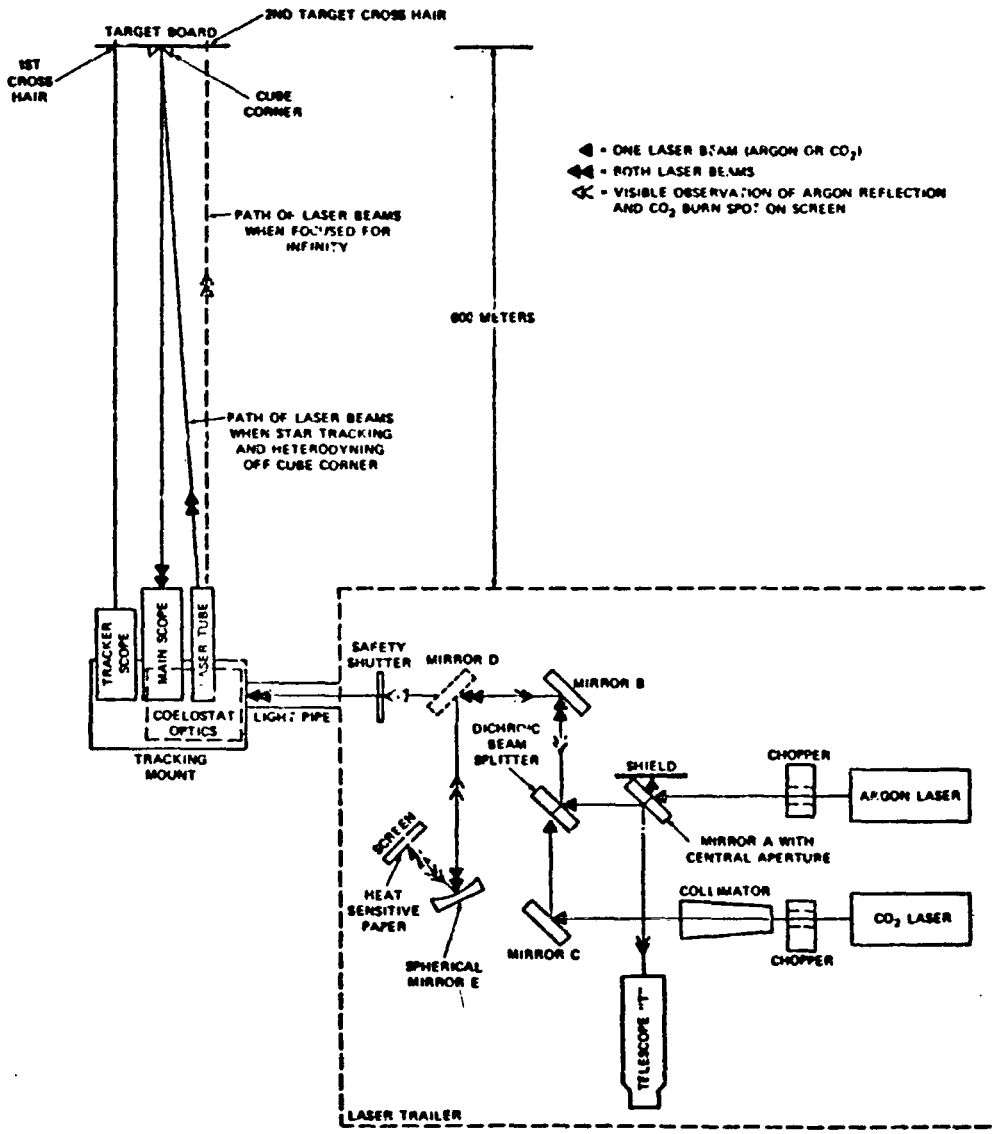

Figure 3-2. Total Optical Test System

an actual balloon flight, similar alignment procedures could be carried out using the balloon as a target roughly approximating an object at infinity.

3.3 Alignment of Ground Station to Startracker Optics

After following the procedures described in Section 3.2, final adjustments of the ground station optics were made. The mount was placed in the autotrack mode using as a source the "star" produced by the reflection of the chopped Argon beam off of a 5 cm diameter cube corner at a range of 0.6 Kilometers. The Mirror M1 on the ground station was adjusted until the Argon "star" appeared at the center of the crosshairs in eyepiece E (see Figure 2-5). At this point, the chopped CO_2 signal off the cube corner could usually be detected directly by the ground station detector. The output of the detector was amplified by 20 db and displayed on an oscilloscope. The signal was then maximized with respect to Mirror M1 and lens L. The eyepiece was then adjusted, if necessary, to correct for any movement of the Argon image due to the optimization procedures. A typical peak-to-peak signal level at the input to the oscilloscope was 100 millivolts.

In a few rare instances, the CO_2 signal was not observed when the Argon "star" was centered on the crosshairs due to unavoidable thermal and mechanical "drifts" in the optics. If this was the case, the telescope mount was taken out of autotrack and placed in a manual mode. Scanning in the area around the cube corner target usually produced a signal at the CO_2 detector. The CO_2 detector was then "walked" into alignment with the startracker by slowly displacing the scope from the point of maximum signal to the autotrack point while simultaneously adjusting Mirror M1 for maximum signal. This procedure finally resulted in a CO_2 signal when the system was in autotrack and the optimization method described above could then be employed.

Once the signal was optimized, the 5 cm diameter cube corner was replaced by a 0.95 cm diameter cube corner at the same range. This resulted in more accurate tracking by the startracker since the Argon image more closely approximated a "point" source and allowed even finer alignment of the ground station to the startracker optics. However, directly detected CO_2 signal levels at the input to the oscilloscope were quite small (typically 3 millivolts peak-to-peak when optimized and amplified by 20 db) due to the reduced intensity of the return beam resulting from the smaller cube corner diameter.

3.4 Alignment of CO_2 Transmitter with Return Argon Beam

Realignment of the flight package optics was carried out prior to each flight by a method illustrated in Figure 3-3. The flight package startracker locked onto

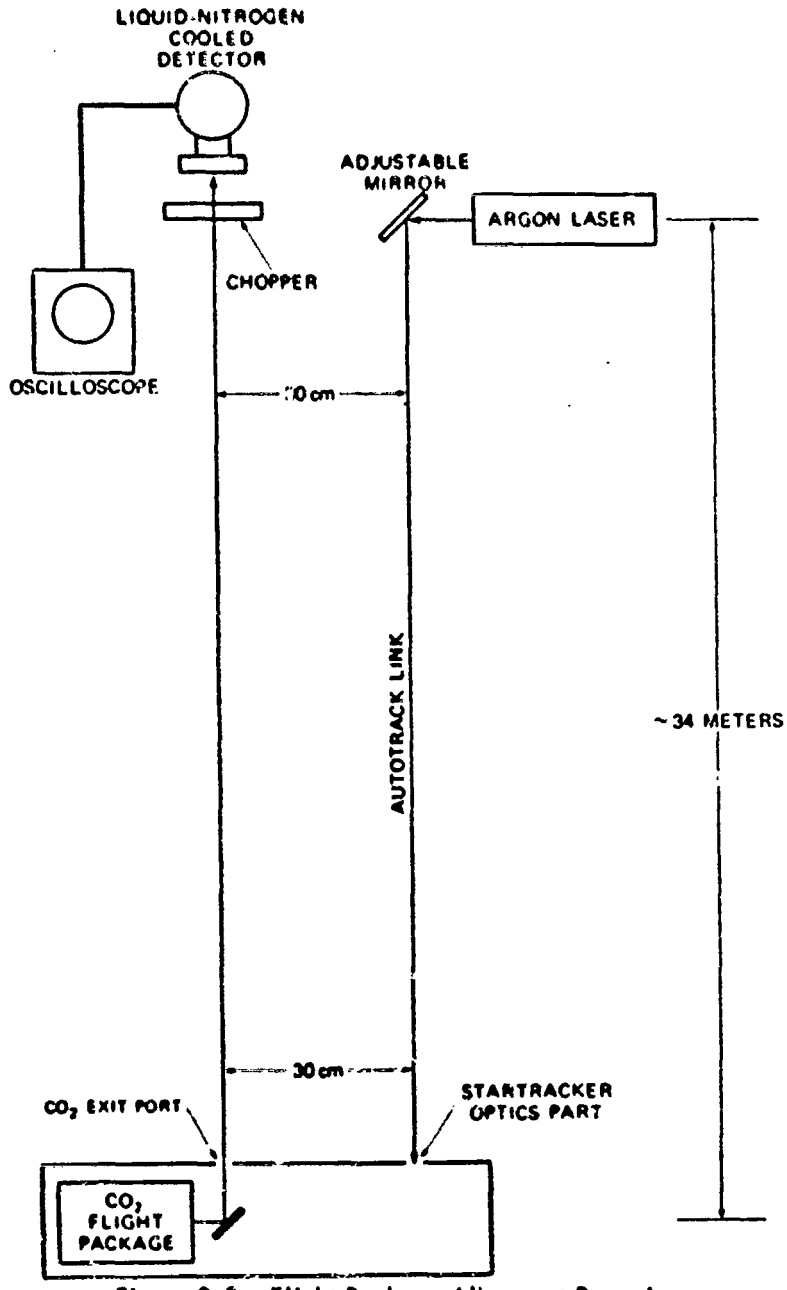

Figure 3-3. Flight Package Alignment Procedure

the "star" provided by a 10 milliwatt Argon laser located approximately 34 meters away. A liquid nitrogen cooled CO_2 detector was displaced from the Argon beam steerer by a distance equal to the displacement between the entrance port for the startracker optics and the exit port for the CO_2 transmitter, about 30 cm. The initial CO_2 beam direction was determined by burning heat sensitive paper and the mirror controlling the direction of the CO_2 beam was adjusted for an initial rough alignment. Fine adjustment was achieved by alternately breaking lock, rotating the package until the signal (chopped) at the CO_2 detector was optimized, adjusting the mounting screws on the laser package and returning to lock. This process was repeated until the signal was optimized with the startracker locked onto the Argon star. This alignment procedure insured that the returning CO_2 beam would be parallel to the outgoing Argon beam to within 0.5 milliradians and hence, the 76 cm diameter scope would be well within the 5 milliradian CO_2 "cone".

3.5 Heterodyning with the Flight Package over the 0.6 Kilometer Test Range

As mentioned previously in Section 2.2.1, the ground station mixer had an effective field-of-view of 8 arcseconds and was aligned such that it focused on the same spatial point as the startracker. Thus, when the tracking mount was in the autotrack mode, the Argon "star" appeared on the crosshairs of the receiver eyepiece. In Section 3.4, however, it was noted that the return Argon beam was displaced from the CO_2 transmitter port by about 30 cm but that the two beams were parallel. At a range of 0.6 kilometers, this displacement amounts to a separation of 0.5 milliradians or 103 arcseconds. Thus, with the system in autotrack, no signal could be observed from the infrared mixer at this short range since the laser was out of the field-of-view of the mixer. The situation was remedied by holding a flashlight at the exit port for the CO_2 transmitter. The signal from the flashlight was easily observed through the eyepiece on the ground station receiver. Mirror M1 on the ground station receiver was then adjusted until the focused white spot was centered on the crosshairs. At this point, the CO_2 signal appeared at the mixer output and heterodyning could begin. After the heterodyning experimentation was terminated, the ground station could then be returned to its original alignment with the startracker by readjusting Mirror M1 until the Argon "star" was again centered on the crosshairs.

4. THEORETICAL CALCULATIONS OF SIGNAL STRENGTHS

4.1 Signal Strength from a 5 cm Diameter Cube Corner at a Range of 0.6 Kilometers

The equation for the received signal strength is:

$$S_r = P_T \; T_A \left(\frac{A_{cc} \; T_{cc}}{\pi \; (\theta_T \; R)^2} \right) FI \; T_{TO} \qquad (4\text{-}1)$$

where:

P_T = Transmitter Power = 6.5 watts

T_A = Round Trip Transmission of Atmosphere (1.2 Kilometer Path Length) = 0.5

Acc = Area of Cube Corner = 7.85×10^{-3} m^2

Tcc = Transmission of Cube Corner = 0.90

θ_T = Transmitter Divergence = 1×10^{-3} Radians

R = Range = 0.6×10^3 Meters

T_{TO} = Transmission of Mount and Ground Station Optics (Nine mirrors, one lens, two beam splitters) = 0.15

F_I = Fraction of Power Returned by Cube Corner Intercepted by Receiving Aperture

Since the cube corner returns the incident light directly back on itself, the center of the return beam lies at the center of the laser tube and not at the center of the receiving aperture which is displaced 48.2 cm away from the laser tube center. The fraction of power intercepted by the receiving aperture is calculated with the aid of Figure 4-1 and the following equation for the radius rc of the return beam.

$$ro = \theta ccR = \left(\frac{1.22 \lambda R}{D}\right) \qquad (4\text{-}2)$$

where:

θcc = Cube Corner Divergence

λ = Wavelength of the Radiation = 10.6×10^{-6} meters

D = Diameter of the Cube Corner = 5×10^{-2} meters

and

R = Range = 0.6×10^3 meters

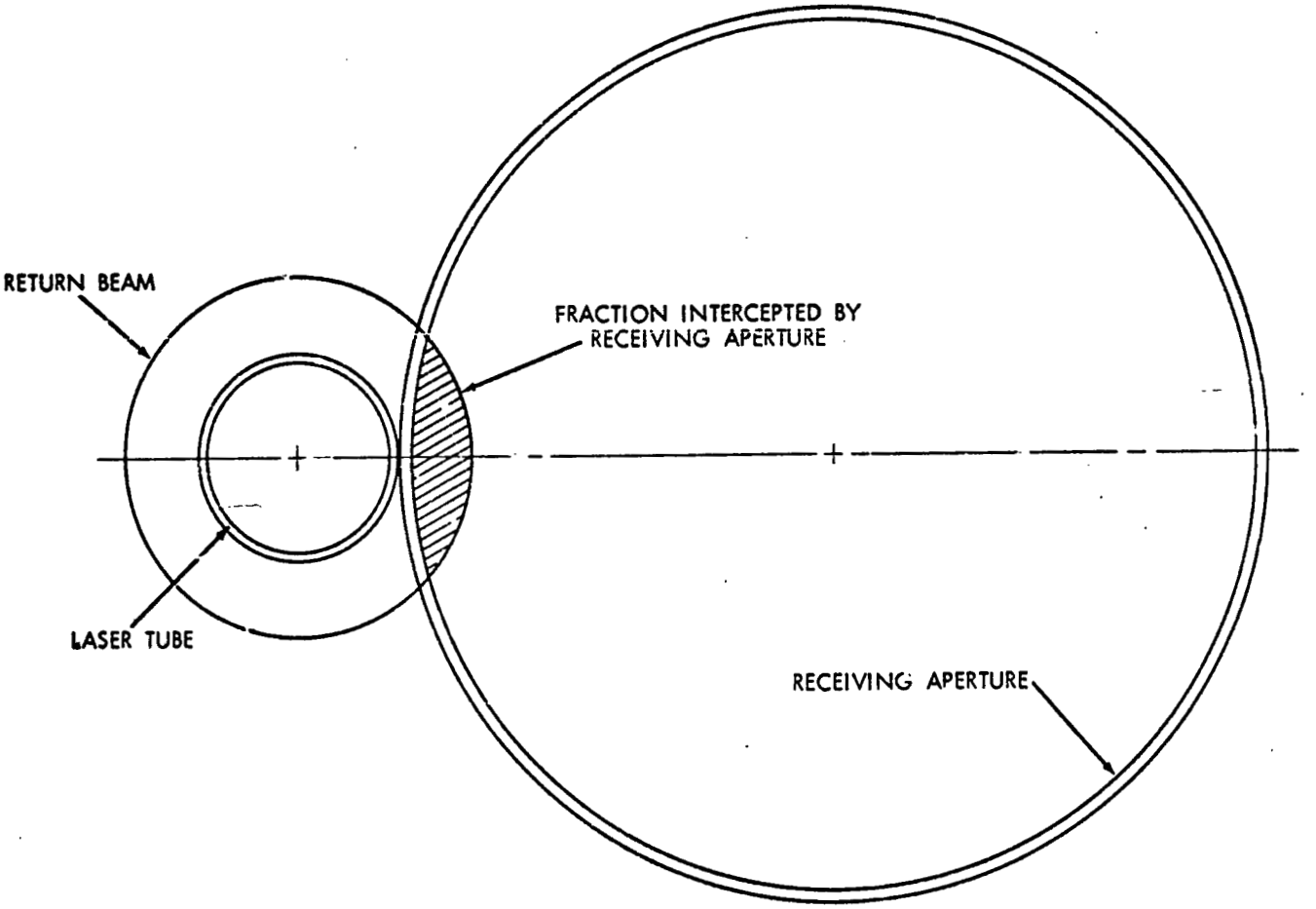

Figure 4-1. Return From a Five cm Diameter Cube Corner

Thus we obtain a value ro = 15.5 cm. Only a small fraction of the returning radiation is intercepted by the receiving aperture. This fraction is calculated to be approximately 0.1. From equation 4-1, we calculate a value of 3×10^{-4} watts for the received signal power assuming perfect pointing.

4.2 Signal Strength from a 0.95 cm Diameter Cube Corner at a Range of 0.6 Kilometers

We substitute Acc = 2.84×10^{-4} m in equation 4-1 and D = 0.95×10^{-2} m in equation 4-2. This gives ro = 81.5 cm for the radius of the returning beam and a value of 0.25 for F_I. The resulting signal strength at the mixer is 2.7×10^{-5} watts.

4.3 Signal Strength from a 30 cm Diameter Flat at a Range of 0.7 Kilometers

The equation for received signal strength is:

$$S_R = P_T \left(\frac{A_M}{\pi (\theta_T R)^2}\right) T_A \, T_{TO} \left(\frac{A_R}{\pi (\theta_T R)^2}\right)$$

where:

P_T = Transmitter Power = 1 Watt

A_M = Mirror Aperture = 0.283 m^2

θ_T = Transmitter Divergence = 2.5×10^{-3} Radians

R = Range = 0.7 Kilometers

A_R = Receiver Aperture = 0.455 m^2

T_A = Round-trip Atmospheric Transmission at 10.6 Micrometers = 0.6

T_{TO} = Transmission of Total Optics (Ten mirrors, one lens, two beam splitters) = 0.14

Substitution of the above parameters gives an expected signal strength of 1.1×10^{-3} watts.

4.4 Signal Strength from a Balloon-Borne CO_2 Transmitter at Ranges Between 0.6 and 30 Kilometers

The equation for received signal strength is now:

$$S_R = P_T \left(\frac{A_R}{\pi (\theta_T R)^2} \right) T_A \; T_{TO}$$

where:

P_T = Transmitter Power = 0.5 Watts

A_R = Receiver Aperture = 0.455 m^2

θ_T = Transmitter Divergence = 2.5×10^{-3} Radians

R = Range

T_A = Atmospheric Transmission at 10.6 Micrometers = 0.6

T_{TO} = Transmission of Total Optics (Four mirrors, 2 beam splitters, and a lens) = 0.26

At a range of 15 Kilometers, the expected signal strength is 8.0×10^{-6} watts. At 30 Kilometers, the expected value is 2.0×10^{-6} watts. At the test range value of 0.6 Kilometers, the signal strength would be 5.0×10^{-3} watts.

5. RESULTS

The CO_2 flight package flew on four separate occasions. On the first two flights, valve leaks caused the balloons to land prematurely so that very little time was available for experimentation. On the last two flights, the balloons were launched outside the 32 kilometer Argon lock-up range with the expectation that the prevailing high-altitude winds would carry the flight package over the ground station. Unfortunately, in both instances, the balloon drifted even farther down range and hovered at typical ranges of 57 kilometers and at elevation angles below 20 degrees. For reasons given in Section 2.1 either of these factors would make a double Argon lock-up virtually impossible to achieve. Without the latter, attempts at heterodyning with the flight package could not even be initiated. Nevertheless, valuable information on the performance of the CO_2 transmitter in flight was obtained from the telemetry readout of the flight package bolometer output. Also, the heterodyne experiments over the horizontal range,

in addition to providing an opportunity to develop valuable field alignment techniques and to obtain data related to signal strengths over long-range paths, pointed out certain areas where system improvement is needed. These are discussed in the following sections.

It should be mentioned that, the flight package was able to lock onto the ground-based Argon "star" for a brief period in spite of the extreme range and low elevation angle, but the ground-based tracker could not lock onto the much weaker return beam. While this allowed atmospheric propogation measurements to be made on the Argon beam using on-board detectors with manual tracking of the flight package (the latter data is reported elsewhere), the manual tracking error was too great to allow meaningful attempts to establish a lock-up between the CO_2 transmitter and the local oscillator due to the narrow field-of-view (±4 arcseconds) of the ground-based CO_2 mixer. (In the automatic tracking mode, the worst case root-mean-square peak-to-peak tracking deviation was measured to be about 3 arcseconds. Under optimum conditions, the same quantity was measured to be about 0.6 arcseconds.) In addition, the star-tracker interfered with the operation of the CO_2 transmitter as discussed in Section 5 2.

5.1 Heterodyne Beats Over the Horizontal Range

A number of heterodyne experiments were carried out over a horizontal range of approximately 0.6 kilometers. Reflections from flats and cube corners provided the transmitter beam for some of these experiments which utilized the optical system shown previously in Figure 3-2. In addition, heterodyne beats were obtained from the flight package over the horizontal range with both startrackers locked onto their respective "stars". The expected optimum signal strengths were calculated in Sections 4.1 through 4.4.

In contrast to the highly stable heterodyne beat usually obtained in the laboratory, the beats observed in the field experiments were oscillatory in nature as is evident from the accompanying figures.

Figure 5-1 is the heterodyne beat obtained from a 30 cm flat at a range of 0.7 kilometers. In this particular experiment, the AIL package was employed and the tracker mount power was turned off. In subsequent experiments, when the tracker mount power was turned on, the AIL package was unable to even hold the beat on the RF spectrum analyzer screen for a reasonable length of time.

In the remaining set of photographs, the back-up system was utilized with the tracker mount power on. Figure 5-2 shows the beat from a 0.95 cm diameter cube corner at a range of 0.6 kilometers, while Figure 5-3 shows the beat

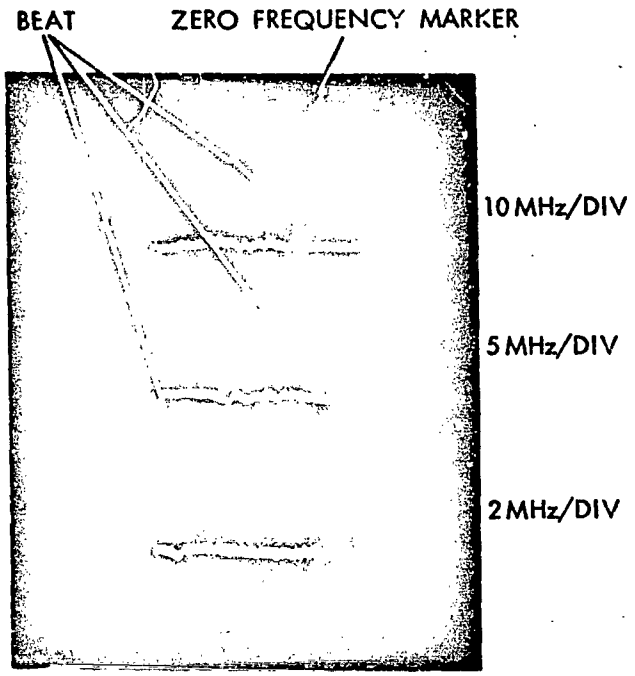

Figure 5-1. Heterodyne Beat From 30 cm Flat

from the flight package over the same horizontal range. As is evident from the oscilloscope traces, the beats are again highly oscillatory. It has since been determined that the oscillation is due primarily to AC noise pickup in the high gain loops.

The sources for this noise and the manner in which its deleterious effect on the stability of the laser beat frequency might be eliminated is discussed in the final section of this report. In spite of the unstable beat frequencies, the observed signal strengths and the stability of the optical alignment were encouraging. It should be mentioned that local oscillator power on the detector could be increased by almost a factor of ten without exceeding the detector limits. This would result in signal strengths almost 10db larger than those reported here.

5.2 Performance of the Flight Package

The performance of the laser transmitter was monitored by a telemetry readout of the bolometer onto a strip chart recorder. As described previously in Section 2.3.2, a non-zero reading is obtained only if the laser is operating on the P(20) molecular line. The level of the reading is an indication of the

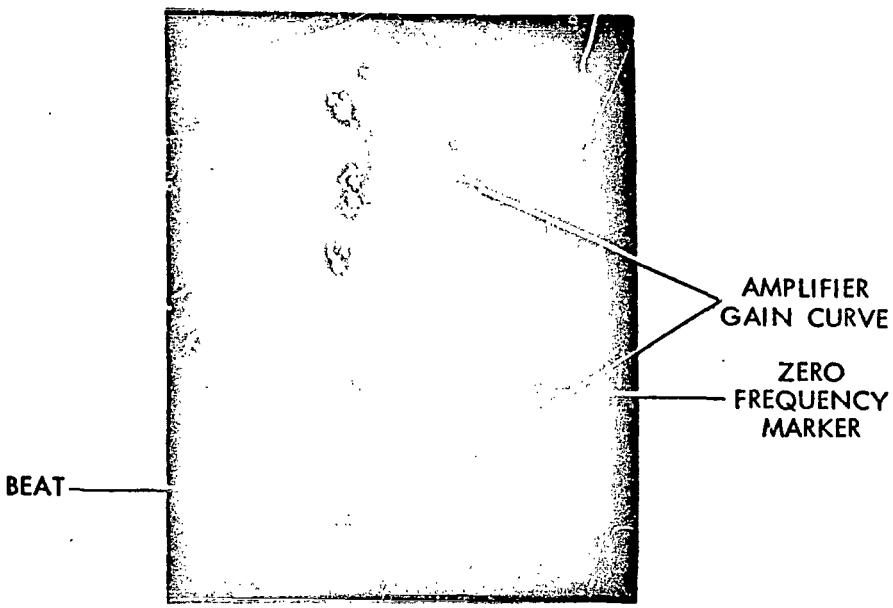

Figure 5-2. Heterodyne Beat From 0.95 cm Diameter Cube Corner

amount of power degradation over an extended period of time. Figure 5-4 displays portions of actual in-flight readings of the bolometer response. Figure 5-4a shows a typical warm-up period. At the extreme right of the figure, there is a sharp rise in the bolometer output as the laser control electronics secures operation on the P(20) molecular line of CO_2 seconds after the laser power is turned on by telemetry command. The ambient temperature was recorded to be -60° at an altitude of 63,000 feet. As the system attempts to reach thermal equilibrium with its environment, the voltage reading rises due to the fact that the incident laser energy on the active flake is causing the temperature to rise more quickly than in the compensator flake. At the same time, the laser cavity length is changing due to temperature variations, causing the P(20) peak to move with respect to the PZT voltage axis in Figure 2-11. As the peak on which dither stabilization has been acquired approaches the extreme range of the PZT tuner driver, the level sensing and inhibit circuit (Section 2.3.2) breaks lock, causing a sharp drop in voltage. This occurs several times before operation is secured on a P(20) line at a different point of the PZT voltage range as evidenced by the lower voltage level of approximately one minute duration seen prior to the first "reset". As the cavity length continues to drift, this lock is broken and the system alternately reacquires and breaks lock.

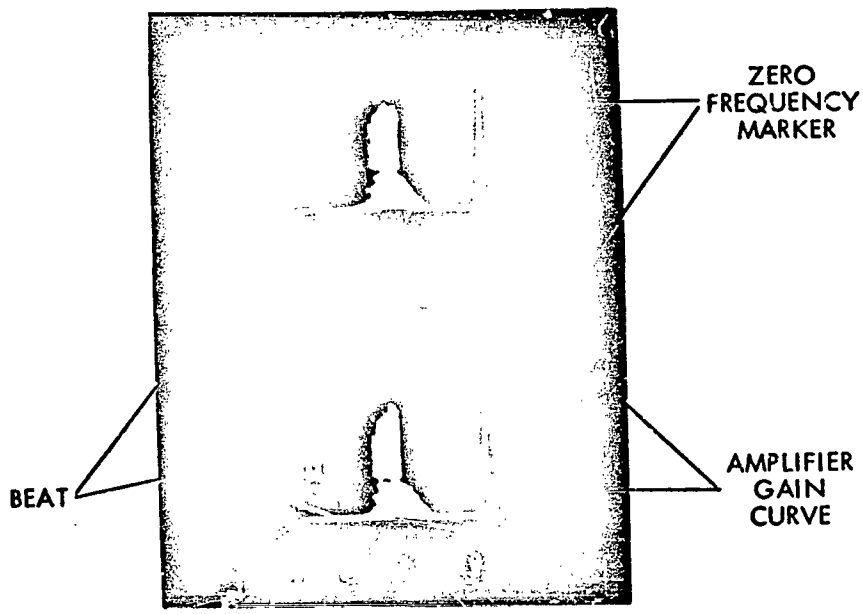

Figure 5-3. Heterodyne Beat From Flight Package

At the end of the first 256 second period, the chopper described in Section 2.3.2 blocks the beam to enable the laser control circuitry to cancel the spurious voltage resulting from the aforementioned thermal drifts. At this point, the 0.5 Hz ramp voltage is reapplied to the PZT, and dither stabilization is re-established on the P(20) line. The second reset shows the nulling of another small positive error after which thermal equilibrium is attained. A half-hour period of normal operation is shown in Figure 5-4b where all power on the payload was turned off except for the laser package and telemetry.

The in-flight performance of the CO_2 transmitter package was normal except for what seems to be an interface problem with the startracker circuitry. During a typical balloon flight, the laser control electronics were unaffected by the simultaneous operation of the other on-board-circuitry such as telemetry, the servo systems for the azimuth and elevation axes, on-board detectors, or startracker power circuitry as demonstrated in Figure 5-4b and the period in Figure 5-4c prior to "Payload Lock-up." However, when the on-board star-tracker actually locked onto the ground-based Argon "star" the operation of the CO_2 transmitter on the P(20) molecular line was interfered with. This effect appeared as a series of rapid "resets" on the strip chart recorder output of the bolometer response as shown in Figure 5-4c. An attempt to duplicate the latter

Figure 5-4(a)

Figure 5-4(b)

Figure 5-4(c)

effect on the ground by the application of mechanical shock and/or movement of the flight package over rough terrain on the back of a truck, with both startrackers locked, failed. No interference with P(20) line operation was observed, although high frequency noise of a few millivolts amplitude was observed on the DC input lines to the transmitter package when the system was in autotrack. Placing the transmitter on its own batteries and the elimination of possible ground loops in the flight package had no effect on the interference in flight.

6. DISCUSSION

6.1 Sources of Noise

An analysis of noise in the ground station AFC loop revealed that the Lansing DC amplifier passed harmonics of 60 cycles directly into the local oscillator PZT from the external line power source. The magnitude of these harmonics were of the order of 5 millivolts at the PZT. As the gain of the loop was increased to improve the lock, large oscillations at 120 and 240 Hz (on the order of two volts) were observed at the output of the discriminator before an effective lock could be established. These oscillations occurred simultaneously with the onset of oscillations in the heterodyne beat frequency observed on an RF spectrum analyzer. The frequency response of the Lansing, which, unfortunately, was the only DC amplifier available at the time of flight, was barely sufficient to track the noise it was introducing into the system as is evident from Figure 2-7(k).

A source of noise in the 6 KHz range was the chopper in the DC-DC converter which was used to power the local oscillator. Because of power limitations on the tracking mount, it was necessary to supply DC voltage to the DC-DC converter and the AFC circuit from the same source. This allowed the 6.1 kilohertz frequency to enter the high-gain AFC loop over the DC supply lines. Capacitive coupling to ground at the output of the DC-DC converter improved the situation only slightly. Noise at these frequencies can be important since recent experimentation reveals that the Double-Disc Bender Piezoelectric transducers used to tune the local oscillator in the present experiment exhibit resonances in precisely this frequency range. The exact resonant frequency will depend not only on the characteristics of the PZT but also on the manner in which it is mounted and the amount of loading caused by the mirror.

The peak-to-peak shift in beat frequency as a result of a sinusoidal voltage applied to a Double-Disc Bender Piezoelectric transducer on the local oscillator is plotted as a function of the applied frequency in Figure 6-1. An extremely large resonant peak in the 3.7 KHz range is evident from the plot. The Double-Disc Bender PZT requires fewer volts per megahertz of laser frequency shift

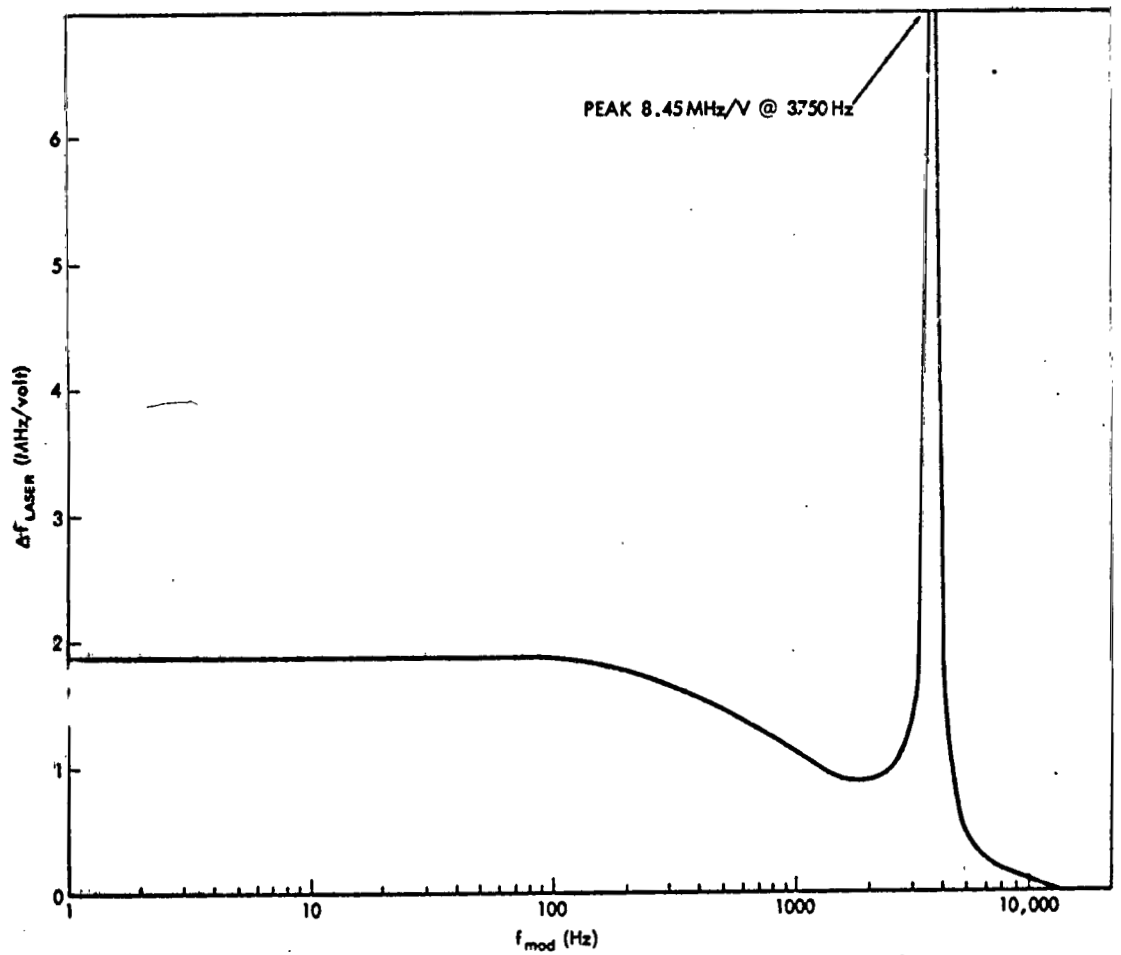

Figure 6-1. Double Disc Bender in Honeywell (Flow System)

than the standard ceramic disk whose typical frequency response is given in Figure 6-2. The difference in voltage requirements is evident from the two graphs. It should be noted that the ceramic disc is characterized by much smaller resonances in the region beyond 14 KHz.

Radiative pickup was a serious problem since the tracking mount behaved like an antenna for frequencies in the 15 to 50 MHz range. Considerable noise in the neighborhood of the 20 MHz center frequency appeared at the output of the preamplifier stage in the AFC loop when transmission of the IF beat frequency signal through the tracking mount slip rings was attempted. This noise was capable of generating false error voltages in the discriminator which further reduced the lockup capability of the system. Taking the signal directly from the preamplifier output without going through the mount slip rings seemed to eliminate this radiative pickup.

The tracker mount servo system which operates at 400 Hz also had an effect on the local oscillator frequency. An amplitude modulation at 400 Hz in the output of the local oscillator when the servo system was turned on indicated an obvious electrical interaction between the laser and the tracking mount which seemed to be more important than mechanical vibration. It is believed that small sinusoidal voltages at 400 Hz appeared at the input to the local oscillator PZT as a result of ground loops. This would result in a modulation of the resonant frequency of the cavity and a resulting amplitude modulation of laser output power due to the shape of the CO_2 Doppler linewidth.

6.2 Suggested Guidelines for Future Systems

Since even low level noise appears to have a significant effect on the performance of the high-gain ground station electronics, precautions must be taken to eliminate mechanical and electrical disturbances. To this end, it is suggested that future systems have no mechanical or electrical contact with the tracking mount which is the major source of vibration and electrical noise. An alternative approach would be the use of a coelostat or similar device to transfer the beam to an optical table inside an adjacent trailer or to a ground station network below the mount. The local oscillator could then be powered by conventional supplies and the need for small DC-DC converters, which introduce kilohertz range noise into the feedback loop, would then be eliminated along with several grounding problems.

The weak link in the ground station electronics is the Lansing DC amplifier. Efforts must be made to build an amplifier with a much flatter frequency response curve and a bandpass to at least several hundred cycles. Furthermore, it is suggested that the amplifier be powered by a DC voltage to eliminate low frequency AC ripple at the input to the piezoelectric transducer.

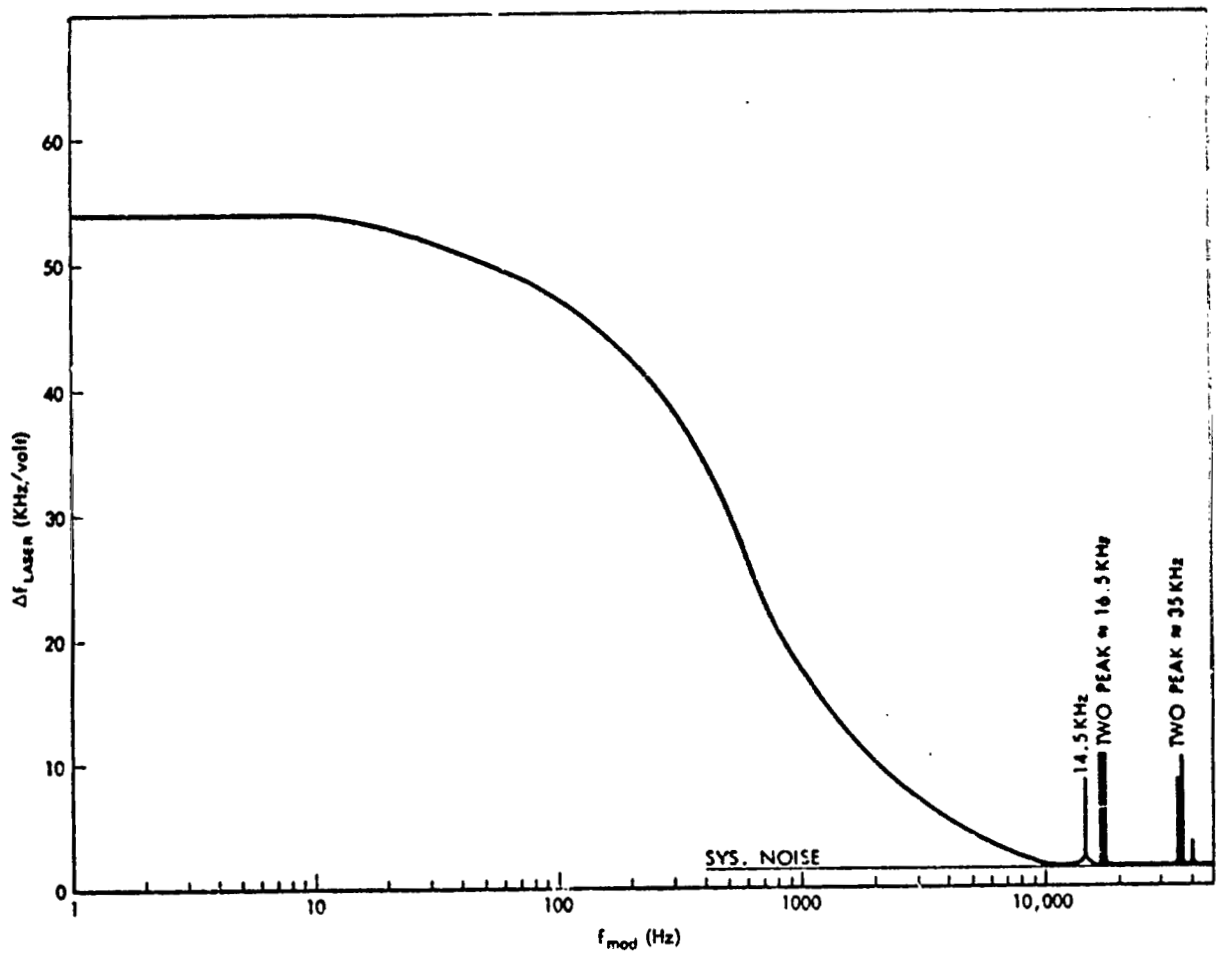
60
50
40
30
20
10
0
Δf_{LASER} (KHz/volt)
1
10
100
1000
10,000
f_{mod} (Hz)
SYS. NOISE
14.5KHz
TWO PEAK ≈ 16.5KHz
TWO PEAK ≈ 35KHz

Figure 6-2

Piezoelectric transducers which do not have potentially troublesome resonances or mounting techniques to eliminate the resonances should be sought. Although a frequency response similar to that shown in Figure 6-2 is more than adequate, the voltage required to drive this type of transducer makes it unattractive for spacecraft use.

A grating and bolometer network similar to that used on the flight package should be installed in the ground station to monitor the frequency of the local oscillator. Furthermore the field-of-view of the ground-based CO_2 detector should be enlarged. These changes would greatly facilitate the search for a heterodyne beat during an actual flight situation.

Further research into the causes of the startracker interference with the CO_2 flight package operation is necessary to determine if mere filtering of the DC power lines leading to the package is sufficient to eliminate the interface problem.

Acknowledgement

The laser frequency control system and mirror mounts employed in the flight package were developed by the Sylvania Electronic Systems — Western Division. That organization also fabricated (to GSFC design) and processed the laser tubes used in the ground station and flight package.

The ground station receiver electronics were developed by AIL, a division of Cutler-Hammer, Inc.

The authors wish to acknowledge the supporting efforts of A. DiNardo of AIL, R. S. Reynolds of Sylvania, and the Optical Techniques Section at Goddard Space Flight Center.

APPENDIX A

OPTICAL HETERODYNING

In a heterodyning experiment, the electric field incident on the mixer is given by:

$$\vec{E}(t) = \vec{E}_T \cos 2\pi \nu_T t + \vec{E}_{LO} \cos (2\pi \nu_{LO} t + \phi)$$

where the transmitter and local oscillator frequencies ν_T and ν_{LO} are equal to the P(20) molecular line frequency (~28 THz) to within the latter's Doppler bandwidth (±50 MHz). We have also allowed for a phase difference ϕ. The power into the mixer is proportional to the electric field squared or

$$P(t) = E_T^2 \cos^2 (2\pi \nu_T t) + E_{LO}^2 \cos^2 (2\pi \nu_{LO} t + \phi)$$

$$+ 2 \vec{E}_T \cdot \vec{E}_{LO} \cos (2\pi \nu_T t) \cos (2\pi \nu_{LO} t + \phi)$$

By a few well-known trigonometric identities this can be rewritten as

$$P(t) = \frac{E_T^2 + E_{LO}^2}{2} + \frac{E_T^2}{2} \cos\left[2\pi (2\nu_T) t\right] + \frac{E_{LO}^2}{2} \cos\left[2\pi (2\nu_{LO}) t + 2\phi\right]$$

$$+ \vec{E}_T \cdot \vec{E}_{LO} \cos\left[2\pi (\nu_T + \nu_{LO}) t + \phi\right] + \vec{E}_T \cdot \vec{E}_{LO} \cos\left[2\pi (\nu_T - \nu_{LO}) t - \phi\right]$$

Ignoring the DC component, we can see that all of the above items are oscillatory at frequencies on the order of 56 THz (twice the P(20) frequency) except for the last term corresponding to our Intermediate Frequence (IF). The latter is the only frequency which lies within the response bandwidth of the mixer and is limited to approximately 50 MHz by the Doppler bandwidth of the molecular line. The phase ϕ of the wave is unimportant since its value only depends on the time origin chosen. Note, however, that the amplitude of the IF frequency depends on the scalar product of E_1 and E_2. Thus, no signal is detected if the polarization of the two beams are orthogonal at the mixer and we get maximum signal if they are parallel. This must be taken into consideration in the design of a heterodyne system.

END

DATE

FILMED

APR 30 1973